Journal of Scientific Computing (2020) 85:25
https://doi.org/10.1007/s10915-020-01337-3

Multiscale Simulation for the System of Radiation Hydrodynamics

Wenjun Sun[1] · Song Jiang[1] · Kun Xu[2] · Guiyu Cao[2]

Received: 2 March 2020 / Revised: 8 August 2020 / Accepted: 8 October 2020

Abstract
This paper aims at the simulation of multiple scale physics for the system of radiation hydrodynamics. The system couples the fluid dynamic equations with the radiative heat transfer. The coupled system is solved by the gas-kinetic scheme (GKS) for the compressible inviscid Euler flow and the unified gas-kinetic scheme (UGKS) for the non-equilibrium radiative transfer, together with the momentum and energy exchange between these two phases. For the radiative transfer, due to the possible large variation of fluid opacity in different regions, the transport of photons through the flow system is simulated by the multiscale UGKS, which is capable of naturally capturing the transport process from the photon's free streaming to the diffusive wave propagation. Since both GKS and UGKS are finite volume methods, all unknowns are defined inside each control volume and are discretized consistently in the updates of hydrodynamic and radiative variables. For the coupled system, the scheme has the asymptotic preserving property, such as recovering the equilibrium diffusion limit for the radiation hydrodynamic system in the optically thick region, where the cell size is not limited by photon's mean free path. A few test cases, such as radiative shock wave problems, are used to validate the current approach.

Keywords Radiation hydrodynamics · Asymptotic preserving · Gas kinetic scheme · Unified gas kinetic scheme · Radiative shock wave

✉ Kun Xu
makxu@ust.hk

Wenjun Sun
sun_wenjun@iapcm.ac.cn

Song Jiang
jiang@iapcm.ac.cn

Guiyu Cao
gcaoaa@connect.ust.hk

[1] Institute of Applied Physics and Computational Mathematics, No. 2, FengHao East Road, HaiDian District, Beijing 100094, China

[2] Department of Mathematics, Hong Kong University of Science and Technology, Clear Water Bay, Kowloon, Hong Kong

Published online: 19 October 2020

1 Introduction

This paper is about the construction of an asymptotic preserving numerical scheme for radiation hydrodynamics. Radiation hydrodynamics describes radiative transport through a fluid with coupled momentum and energy exchange. The system is routinely used in high energy density physics, astrophysics, the inertial confinement fusion (ICF), and other flows with very high temperature. For radiation hydrodynamics, radiation propagates through a moving hydrodynamic material. Due to the moving velocity of the material, the thermal radiative transfer equation includes relativistic material-motion correction whenever the radiation momentum deposition has a measurable impact on the material dynamics. The correction is applicable for flow with moving velocity being much smaller than the speed of light. Following the works of [1–3], we adopt Morel's radiation hydrodynamic model in this paper, which is denoted as $MM(\theta)$ model in Eq. (2.1) with θ as a free parameter. Morel's system can be viewed as a simplified laboratory-frame formulation. The parameter θ can be chosen based on the numerical method, such as $MM(\theta = 1)$ for a Lagrangian approach and $MM(\theta = 0)$ for the Eulerian one. Based on Morel's model and the consideration of multiple time scales in the radiation hydrodynamic system, the Eq. (2.1) are usually split into time-scale dependent equations of radiation and fluid movement due to the large discrepancy of the fluid velocity and the speed of the light.

Though excellent work has been done separately for the study of radiative transfer [4–13] and fluid dynamics [14,15], the research for the coupled system has only been carried out recently [3,16–20]. The equations of radiation hydrodynamics include explicitly the motion of the background material. For low opacity material, such as the case with small absorption/emission coefficients and small scattering coefficient, the interaction between the radiation and material is weak and the radiation propagates in a transparent way with a particle-type behavior, i.e., the so-called optically thin regime. In this regime, the numerical method for radiation should be able to capture the free streaming transport of photons, such as the upwind approach with a ray tracking technique in SN method. For a high opacity material with large absorption/emission coefficients or large scattering coefficient, the intensive momentum and energy exchange between the radiation and material diminishes photon's mean free path. As a result, the diffusive asymptotic limit in the optically thick regime will appear. In the case with large absorption/emission coefficients, an equilibrium diffusive process for radiation will emerge and the material temperature and the radiation temperature will approach to the same value. In this paper, the unified gas-kinetic scheme (UGKS) will be used to solve the radiative transfer equation for capturing both ballistic and diffusive limits of the photon transport [11–13,21].

For hydrodynamics, the gas-kinetic scheme (GKS) has been developed systematically for compressible flow computations [15,22,23]. The numerical flux in the finite volume GKS is based on a gas evolution process from a kinetic scale particle free transport to a hydrodynamic scale Navier–Stokes flux formulation, where both inviscid and viscous fluxes are recovered from moments of a single time-dependent gas distribution function. In the discontinuous shock region, if the cell resolution is not fine enough to resolve the shock structure, the GKS becomes a shock capturing scheme and the kinetic scale based particle free transport provides numerical dissipation to build a numerical shock transition. In the smooth flow region, the GKS becomes a Lax–Wendroff type central difference scheme for recovering the NS solutions.

For the 1D radiation hydrodynamic system in [17], an implicit–explicit (IMEX) method is constructed to solve the Euler equations coupled with gray radiative transfer. In such an

algorithm, the fluid advection component is treated explicitly, whereas the radiation transport and energy exchange components are treated implicitly. Based on the second-order Godunov method [24], an entirely explicit scheme for RH was developed and the time step in the scheme is limited by the time scale of radiative transport.

In this paper we will construct a scheme for the radiation hydrodynamic system by coupling UGKS with GKS uniformly in all regimes. Since both GKS and UGKS are finite volume method, all flow and radiation variables are defined as cell averages. The discretization for both hydrodynamics and radiative evolution can be done consistently. The constructed scheme has the asymptotic preserving (AP) property for the radiation part, and the equilibrium diffusion limit can be obtained automatically by UGKS in the optically thick region.

In this paper, Sect. 2 is the introduction of radiation hydrodynamic system. In Sect. 3, the details of the numerical scheme for the coupled system are presented. In Sect. 4, the asymptotic preserving property of the scheme is proved mathematically. The numerical examples are presented in Sect. 5 to validate the scheme. Section 6 is the conclusion.

2 Radiation Hydrodynamics

For radiation hydrodynamics, when the radiation momentum deposit has a measurable impact on the material dynamics, the thermal radiative transfer equation requires the correction due to the material velocity. The modification is needed even for the case where the speed of flow is much smaller than the speed of light. Under such a condition, the $MM(\theta)$ model [3] for the coupled radiation and hydrodynamics is adopted in the current study. The equations include non-relativistic, inviscid, single-material compressible hydrodynamics and the thermal radiation transport,

$$\begin{cases} \partial_t \rho + \nabla \cdot (\rho \vec{v}) = 0, \\ \partial_t (\rho \vec{v}) + \nabla \cdot (\rho \vec{v} \otimes \vec{v}) + \nabla p = -\frac{1}{c} \int \vec{\Omega} S d\vec{\Omega}, \\ \partial_t (\rho E) + \nabla \cdot [\vec{v}(\rho E + p)] = -\frac{1}{\epsilon} \int S d\vec{\Omega}, \\ \frac{\epsilon}{c} \frac{\partial I}{\partial t} + \vec{\Omega} \cdot \nabla I + \epsilon \nabla \cdot (\theta \vec{\beta} I) = -\frac{\sigma_t}{\epsilon} I + (\frac{\sigma_t}{\epsilon} - \epsilon \sigma_s) \frac{1}{4\pi} acT^4 + \frac{\epsilon \sigma_s}{4\pi} cE_r \\ \quad -\frac{1}{4\pi} \sigma_t \vec{\beta} \cdot \left[\vec{F}_r - \left(\frac{4}{3} - \theta \right) \epsilon E_r \vec{v} \right] + \frac{3}{4\pi} \left(\frac{4}{3} - \theta \right) \sigma_t E_r \vec{\Omega} \cdot \vec{v} \triangleq S. \end{cases} \tag{2.1}$$

Here ρ is the mass density, T the material temperature, $\vec{v}$ the fluid velocity, and $\rho E = \frac{1}{2}\rho |\vec{v}|^2 + \rho e$ is the total material energy. In order to close the equations, the equation-of-state (EOS) $p = p(\rho, T)$ and the material internal energy $e(\rho, T)$ have to be provided. And I is the radiation intensity, which is a function of space, time, angle direction $\vec{\Omega}$, and radiation frequency. For simplicity, in this paper we only consider the gray case, where the intensity is averaged over the radiation frequency. In the above equations, c is the speed of light and $\vec{\beta} \equiv \frac{\vec{v}}{c}$. The S term represents the interaction between the radiation and material in the radiation hydrodynamic system, a is the radiation constant, σ_s is the coefficient of scattering, σ_t is the total coefficient of absorption, and ϵ is the factor of scaling. The free parameter θ is related to the correction due to the material motion. The value of θ varies according to the numerical scheme. For the Lagrangian formulation with moving mesh following the fluid velocity, $\theta = 1$ is used. In the Eulerian formulation, $\theta = 0$ is adopted for the lab-frame, while the case $\theta = 4/3$ can be viewed as an approximate comoving-frame treatment. The functions E_r and $\vec{F}_r$ are the radiation energy and radiation flux respectively, which are given

by

$$E_r = \frac{1}{c}\int I d\vec{\Omega}, \quad \vec{F}_r = \int \vec{\Omega} I d\vec{\Omega}.$$

The momentum and energy deposition from radiation on hydrodynamics are computed by angle integrations on the right hand sides of the second and third equations in (2.1). It is straightforward to derive the corresponding total momentum and energy equations, which are given by

$$\begin{cases} \partial_t(\rho\vec{v} + \frac{\epsilon}{c^2}\vec{F}_r) + \nabla\cdot(\rho\vec{v}\otimes\vec{v} + \frac{\epsilon\theta}{c^2}\vec{v}\otimes\vec{F}_r + \bar{\bar{P}}) + \nabla p = 0, \\ \partial_t(\rho E + E_r) + \nabla\cdot[\vec{v}(\rho E + \theta E_r + p) + \frac{1}{\epsilon}\vec{F}_r] = 0, \end{cases} \tag{2.2}$$

and $\bar{\bar{P}}$ is the radiation pressure tensor calculated by

$$\bar{\bar{P}} = \frac{1}{c}\int \vec{\Omega}\otimes\vec{\Omega} I d\vec{\Omega}.$$

The system (2.1) has the property that it will approach to the equilibrium diffusion limit equations for any choice of θ as the parameter ϵ approaching to 0 in the optically thick region. This can be seen by expanding the dependent variables as a power series of ϵ,

$$\begin{cases} \rho = \sum_{i=0}^{\infty}\rho^{(i)}\epsilon^i, \quad \vec{v} = \sum_{i=0}^{\infty}\vec{v}^{(i)}\epsilon^i, \\ T = \sum_{i=0}^{\infty}T^{(i)}\epsilon^i, \quad I = \sum_{i=0}^{\infty}I^{(i)}\epsilon^i, \end{cases} \tag{2.3}$$

and comparing the terms of equal powers. Substituting the expansions in (2.3) into the governing equations (2.1), the $O(\epsilon^{-1})-$terms of the fourth equation in (2.1) give

$$I^{(0)} = \frac{1}{4\pi}ac(T^{(0)})^4, \tag{2.4}$$

followed by

$$E_r^{(0)} = a(T^{(0)})^4, \quad \vec{F}_r^{(0)} = 0, \quad \bar{\bar{P}}^{(0)} = \frac{1}{3}a(T^{(0)})^4\bar{\bar{\mathbf{D}}}, \tag{2.5}$$

where $\bar{\bar{\mathbf{D}}}$ is the identity matrix. There are no $O(\epsilon^{-1})-$terms in the first two equations of (2.1). And the $O(\epsilon^{-2})$ and $O(\epsilon^{-1})-$terms in the third equation of (2.1) are consistent with the above Eqs (2.4) and (2.5).

Using Eqs (2.4) and (2.5) again, the $O(\epsilon^0)-$terms in the fourth equation of (2.1) reduce to

$$I^{(1)} = \frac{1}{4\pi}ac(T^{(1)})^4 - \frac{c}{\sigma_t^{(0)}}\vec{\Omega}\cdot\nabla I^{(0)} + \frac{3}{4\pi}\left(\frac{4}{3}-\theta\right)E_r^{(0)}\vec{\Omega}\cdot\vec{v}^{(0)}, \tag{2.6}$$

therefore,

$$E_r^{(1)} = a(T^{(1)})^4, \quad \vec{F}_r^{(1)} = -\frac{c}{3\sigma_t^{(0)}}\nabla E_r^{(0)} + \left(\frac{4}{3}-\theta\right)E_r^{(0)}\vec{v}^{(0)}, \quad \bar{\bar{P}}^{(1)} = \frac{1}{3}a(T^{(1)})^4\bar{\bar{\mathbf{D}}}. \tag{2.7}$$

Finally, the $O(\epsilon^0)-$terms in the first equation of (2.1) and the Eq. (2.2) result in

$$\begin{cases} \partial_t \rho^{(0)} + \nabla \cdot (\rho^{(0)} \vec{v}^{(0)}) = 0, \\ \partial_t (\rho^{(0)} \vec{v}^{(0)}) + \nabla \cdot (\rho^{(0)} \vec{v}^{(0)} \otimes \vec{v}^{(0)} + \bar{\bar{P}}^{(0)}) + \nabla p^{(0)} = 0, \\ \partial_t (\rho^{(0)} E^{(0)} + E_r^{(0)}) + \nabla \cdot [\vec{v}^{(0)} (\rho^{(0)} E^{(0)} + \theta E_r^{(0)} + p^{(0)}) + \vec{F}_r^{(1)}] = 0. \end{cases} \tag{2.8}$$

By substituting $\vec{F}_r^{(1)}$ in (2.7) into (2.8), the equilibrium diffusion system for radiation hydrodynamics can be obtained as follows.

$$\begin{cases} \partial_t \rho^{(0)} + \nabla \cdot (\rho^{(0)} \vec{v}^{(0)}) = 0, \\ \partial_t (\rho^{(0)} \vec{v}^{(0)}) + \nabla \cdot (\rho^{(0)} \vec{v}^{(0)} \otimes \vec{v}^{(0)} + \bar{\bar{P}}^{(0)}) + \nabla p^{(0)} = 0, \\ \partial_t (\rho^{(0)} E^{(0)} + E_r^{(0)}) + \nabla \cdot [\vec{v}^{(0)} (\rho^{(0)} E^{(0)} + \frac{4}{3} E_r^{(0)} + p^{(0)})] = \nabla \cdot (\frac{c}{3\sigma_R} \nabla E_r^{(0)}), \end{cases} \tag{2.9}$$

where σ_R is the Rosseland mean that is equal to $\sigma_t^{(0)}$ here.

This paper will present a scheme with the asymptotic preserving property for the radiation hydrodynamic equations (2.1), such that the numerical scheme for (2.1) will converge to a proper numerical method for (2.9) automatically as the parameter ϵ tends to zero. The details of the method will be presented in the next section.

3 Unified Scheme for the Radiation Hydrodynamic System

In this subsection we introduce the detailed construction of an asymptotic preserving scheme for (2.1). The radiation and fluid parts in Eq. (2.1) will be solved separately. For the fluid dynamics, the gas kinetic scheme (GKS) as a Navier–Stokes (NS) flow solver is used, while the multiscale unified gas-kinetic scheme (UGKS) [11] is employed for the radiative transfer, where two solvers are coupled in the momentum and energy exchanges. Since GKS and UGKS are all finite volume methods, all unknowns are defined inside each control volume, and the discretizations for the hydrodynamics and radiative transfer can be done consistently.

The hydrodynamic and radiative transfer solvers are based on the operator-splitting approach. The purely hydrodynamic part of our scheme targets on the following Euler equations, even though the GKS is intrinsically a NS solver,

$$\begin{cases} \partial_t \rho + \nabla \cdot (\rho \vec{v}) = 0, \\ \partial_t (\rho \vec{v}) + \nabla \cdot (\rho \vec{v} \bigotimes \vec{v}) + \nabla p = 0, \\ \partial_t (\rho E) + \nabla \cdot (\vec{v}(\rho E + p)) = 0. \end{cases} \tag{3.1}$$

The above equations are closed by an ideal gas equation of state (EOS) and internal energy equation:

$$\begin{cases} p = (\gamma - 1)\rho e, \\ e = C_v T, \end{cases} \tag{3.2}$$

where γ is the specific heat ratio and C_v is the heat capacity.

For the radiative transfer, the momentum deposition and energy exchange between radiation and material are included in the coupled equations. The algorithm for radiative transfer solves the following equations:

$$\begin{cases} \partial_t(\rho\vec{v}) = -\frac{1}{c}\int \vec{\Omega} S d\vec{\Omega} = \frac{\sigma_t}{\epsilon c}\left[\vec{F}_r - \left(\frac{4}{3}-\theta\right)\epsilon E_r\vec{v}\right], \\ \partial_t(\rho E) = -\frac{1}{\epsilon}\int S d\vec{\Omega} = \frac{1}{\epsilon}(\frac{\sigma_t}{\epsilon}-\epsilon\sigma_s)(cE_r - acT^4) + \frac{\sigma_t}{\epsilon}\vec{\beta}\cdot\left[\vec{F}_r - \left(\frac{4}{3}-\theta\right)\epsilon E_r\vec{v}\right], \\ \frac{\epsilon}{c}\frac{\partial I}{\partial t} + \vec{\Omega}\cdot\nabla I + \epsilon\nabla\cdot(\theta\vec{\beta}I) = -\frac{\sigma_t}{\epsilon}I + (\frac{\sigma_t}{\epsilon}-\epsilon\sigma_s)\frac{1}{4\pi}acT^4 + \frac{\epsilon\sigma_s}{4\pi}cE_r \\ \quad -\frac{1}{4\pi}\sigma_t\vec{\beta}\cdot\left[\vec{F}_r - \left(\frac{4}{3}-\theta\right)\epsilon E_r\vec{v}\right] + \frac{3}{4\pi}(\frac{4}{3}-\theta)\sigma_t E_r\vec{\Omega}\cdot\vec{v} \triangleq S. \end{cases} \tag{3.3}$$

The solver for the radiative hydrodynamic system is constructed by solving the Eqs (3.1) and (3.3) by GKS and UGKS separately.

3.1 Gas-Kinetic Scheme for Fluid Flow

The compressible Euler equation (3.1) is solved by the GKS [15]. In the finite volume GKS, the interface flux between neighboring cells plays a dominant role for the quality of the scheme. The gas evolution at a cell interface is constructed based on the following kinetic model equation [25]:

$$f_t + \vec{u}\cdot\nabla f = \frac{g-f}{\tau}, \tag{3.4}$$

where $f(\vec{x},t,\vec{u})$ is the gas distribution function and $\vec{u}$ is the particle velocity. The function g is the equilibrium state approached by f through a particle collision time τ. The collision term satisfies the compatibility condition

$$\int \frac{g-f}{\tau}\psi d\Xi = 0, \tag{3.5}$$

where $\psi = (1,\vec{u},\frac{1}{2}(|\vec{u}|^2+|\vec{\xi}|^2))^T$ is the collision invariants, $d\Xi = d\vec{u}d\vec{\xi}$, and $\vec{\xi} = (\xi_1,\ldots,\xi_K)$ is the internal variable.

The connections between the macro quantities $(\rho,\rho\vec{v},\rho E)$ and their fluxes with the gas distribution function f are given by

$$\begin{pmatrix}\rho\\ \rho\vec{v}\\ \rho E\end{pmatrix} = \int \psi f d\Xi, \quad \begin{pmatrix}\nabla\cdot(\rho\vec{v})\\ \nabla\cdot(\rho\vec{v}\bigotimes\vec{v})+\nabla p\\ \nabla\cdot[(\rho E+p)\vec{v}]\end{pmatrix} = \int \psi\vec{u}\cdot\nabla f d\Xi. \tag{3.6}$$

Once the gas distribution f at a cell interface is fully determined, the numerical fluxes can be obtained. In GKS, the boundary distribution function f is evaluated from the integral solution of kinetic model equation (3.4):

$$f(\vec{x},t,\vec{u},\vec{\xi}) = \frac{1}{\tau}\int_0^t g(\vec{x}-\vec{u}(t-t'),t',\vec{u},\vec{\xi})e^{-(t-t')/\tau}dt' + e^{-t/\tau}f_0(\vec{x}-\vec{u}t,\vec{u},\vec{\xi}). \tag{3.7}$$

The initial condition f_0 in the above solution is modeled by

$$f_0 = f_0^l(\vec{x},\vec{u},\vec{\xi})\mathrm{H}((\vec{x}-\vec{x}_s)\cdot\vec{n}) + f_0^r(\vec{x},\vec{u},\vec{\xi})(1-\mathrm{H}((\vec{x}-\vec{x}_s)\cdot\vec{n})),$$

where H is the Heaviside function, f_0^l and f_0^r are the initial gas distribution functions at the left and right sides of a cell interface with a normal direction $\vec{n}$, and $\vec{x}_s$ is the center of the

cell interface. To keep a second-order accuracy, the initial distribution f_0 in space around $\vec{x}_s$ is approximated by piecewise polynomials

$$f_0^{l,r}(\vec{x},\vec{u},\vec{\xi}) = f_0^{l,r}(\vec{x}_s,\vec{u},\vec{\xi}) + (\vec{x}-\vec{x}_x)\cdot\nabla f_0^{l,r}(\vec{x}_s,\vec{u},\vec{\xi}).$$

Without loss of generality, with the assumption of $\vec{x}_s = 0$, for the Euler solution (3.1) the initial distribution functions $f_0^{l,r}(0)$ can be expressed as the Maxwellians,

$$f_0^{l,r}(0) = g_0^{l,r}.$$

The equilibrium distribution functions $g_0^{l,r}$ are

$$g_0^{l,r} = \rho^{l,r}\left(\frac{\lambda^{l,r}}{\pi}\right)^{\frac{K+2}{2}} e^{\lambda^{l,r}(|\vec{u}-\vec{v}^{l,r}|^2+|\vec{\xi}|^2)},$$

which are determined from the distributions of initial macroscopic flow variables $W^l = (\rho^l, (\rho\vec{v})^l, (\rho E)^l)$ and $W^r = (\rho^r, (\rho\vec{v})^r, (\rho E)^r)$. The derivatives $\nabla f_0^{l,r}$, such as in the x_k-direction, are obtained from

$$\begin{pmatrix} \frac{\partial\rho}{\partial x_k}|_{l,r} \\ \frac{\partial(\rho\vec{v})}{\partial x_k}|_{l,r} \\ \frac{\partial(\rho E)}{\partial x_k}|_{l,r} \end{pmatrix} = \int \psi \frac{\partial f_0^{l,r}}{\partial x_k} d\Xi, \quad (k = 1,\ldots,3), \tag{3.8}$$

where the derivatives of the macroscopic variables $(\frac{\partial\rho}{\partial x_k}|_{l,r}, \frac{\partial(\rho\vec{v})}{\partial x_k}|_{l,r}, \frac{\partial(\rho E)}{\partial x_k}|_{l,r})$ are reconstructed with the MUSCL slope limiter [26].

After determining the initial distribution function f_0, the equilibrium state g in the integral solution (3.7) can be expanded in space and time as

$$g = \bar{g} + \nabla\bar{g}\cdot\vec{x} + \frac{\partial\bar{g}}{\partial t}t, \tag{3.9}$$

where $\bar{g}$ is the equilibrium distribution function at a cell interface and is determined by the compatibility condition

$$\int \psi\bar{g}d\Xi = \bar{W} \triangleq (\bar{\rho}, \bar{\rho}\vec{\bar{v}}, \bar{\rho}\bar{E})^T = \int_{\vec{u}\cdot\vec{n}>0} \psi g_0^l d\Xi + \int_{\vec{u}\cdot\vec{n}<0} \psi g_0^r d\Xi.$$

With the following notations

$$a_k^{l,r} = \bar{g}_{x_k}^{l,r}/\bar{g}, \quad A^{l,r} = \bar{g}_t^{l,r}/\bar{g},$$

the spatial derivatives $\bar{g}_{x_k}^{l,r} = (\partial\bar{g}/\partial x_k)|_{l,r} (k = 1,\ldots,3)$ and time derivative $\bar{g}_t^{l,r} = (\partial\bar{g}/\partial t)|_{l,r}$ are obtained from the relations

$$\int \psi a_k^{l,r} d\Xi = \frac{\partial\bar{W}}{\partial x_k}|_{l,r}, \quad \int \psi\left(\sum_{k=1}^{k=3} u_k a_k^{l,r} + A^{l,r}\right) d\Xi = 0.$$

The derivatives for the macroscopic variables for the equilibrium states $\frac{\partial\bar{W}}{\partial x_i}|_{l,r}$ are given by

$$\frac{\partial\bar{W}}{\partial x_k}|_l = \frac{\bar{W}-W^l}{x_k^l}, \quad \frac{\partial\bar{W}}{\partial x_k}|_r = \frac{W^r-\bar{W}}{x_k^r}, \quad (k = 1,\ldots,3),$$

where the $x_k^{l,r}$ denote the left and right cell centers around the cell interface and the cell interface is located at $x = 0$.

Up to now, we have presented the gas kinetic scheme (GKS) for the Eq. (3.1). Then, after updating the flow variables inside each cell, the radiation equation (3.3) will be solved next.

3.2 Unified Gas-Kinetic Scheme for Radiative Transfer

3.2.1 General Formulation

After advancing the fluid variables $(\rho, \rho\vec{v}, \rho E)$ by GKS from time step t^n to t^{n+1}, the fluid density is updated from ρ^n to ρ^{n+1}, but the fluid velocity is updated from $\vec{v}^n$ to the intermediate state $\vec{v}^h$, the same as the total specific energy from E^n to E^h. Therefore, the intermediate specific internal energy and kinetic energy get to e^h and $\frac{1}{2}|\vec{v}^h|^2$, respectively. Based on the updated flow values $(\rho^{n+1}, \vec{v}^h, E^h)$, the radiative transfer equation (3.3) become,

$$\begin{cases} \partial_t(\rho\vec{v}) = -\frac{1}{c}\int \vec{\Omega} S d\vec{\Omega}, \\ \partial_t(\rho E) = -\frac{1}{\epsilon}\int S d\vec{\Omega}, \\ \frac{\epsilon}{c}\frac{\partial I}{\partial t} + \vec{\Omega}\cdot\nabla I + \epsilon\nabla\cdot(\theta\vec{\beta} I) = S. \end{cases} \tag{3.10}$$

For the radiation intensity in the above equations, the discrete ordinate method (DOM) [27] is used to discretize the angular variable $\vec{\Omega}$. The vector $\vec{\Omega}$ in unit sphere is divided into M discrete directions $\vec{\Omega}_m$ with corresponding integration weight ω_m. Then, the above system (3.10) can be rewritten (in discrete directions) as

$$\begin{cases} \partial_t(\rho\vec{v}) = -\frac{1}{c}\sum_{m=1}^{M} \vec{\Omega}_m S_m \omega_m, \\ \partial_t(\rho E) = -\frac{1}{\epsilon}\sum_{m=1}^{M} S_m \omega_m, \\ \frac{\epsilon}{c}\frac{\partial I_m}{\partial t} + \vec{\Omega}_m\cdot\nabla I_m + \epsilon\nabla\cdot(\theta\vec{\beta} I_m) = S_m, \quad m = 1, \ldots, M, \end{cases} \tag{3.11}$$

where S_m is the value of S at the discrete angle calculated from the intensity I_m.

The above equations will be solved by UGKS [11]. In the 2D case, the computational cells are denoted by $\{(x, y) : [x_{i-\frac{1}{2}}, x_{i+\frac{1}{2}}] \times [y_{j-\frac{1}{2}}, y_{j-\frac{1}{2}}]\}$. The discrete conservation laws for the control volume $[x_{i-\frac{1}{2}}, x_{i+\frac{1}{2}}] \times [y_{j-\frac{1}{2}}, y_{j-\frac{1}{2}}]$ over the time interval $[t^n, t^{n+1}]$ for every $\vec{\Omega}_m = (\mu_m, \xi_m)$ $(m = 1, \ldots, M)$ are

$$\begin{cases} \rho_{i,j}^{n+1}(\vec{v}_{i,j}^{n+1} - \vec{v}_{i,j}^{h}) = -\frac{\Delta t}{c}\sum_{m=1}^{M} \vec{\Omega}_m S_{i,j,m}^{n+1}\omega_m, \\ \rho_{i,j}^{n+1}(\hat{E}_{i,j}^{n+1} - E_{i,j}^{h}) = -\frac{\Delta t}{\epsilon}\sum_{m=1}^{M} S_{i,j,m}^{n+1}\omega_m, \\ \frac{\epsilon}{c}\frac{I_{i,j,m}^{n+1} - I_{i,j,m}^{n}}{\Delta t} + \frac{F_{i+\frac{1}{2},j,m} - F_{i-\frac{1}{2},j,m}}{\Delta x_i \Delta y_j} + \frac{G_{i,j+\frac{1}{2},m} - G_{i,j-\frac{1}{2},m}}{\Delta x_i \Delta y_j} = S_{i,j,m}^{n+1}. \end{cases} \tag{3.12}$$

Here $\Delta t = t^{n+1} - t^n$, $\Delta x_i = x_{i+\frac{1}{2}} - x_{i-\frac{1}{2}}$ and $\Delta y_j = y_{j+\frac{1}{2}} - y_{j-\frac{1}{2}}$. The boundary fluxes are given by

$$\begin{aligned}
F_{i+\frac{1}{2},j,m} &= \int_{t^n}^{t^{n+1}} \int_{y_{j-\frac{1}{2}}}^{y_{j+\frac{1}{2}}} \mu_m I_{i+\frac{1}{2},j,m} dy dt + \int_{t^n}^{t^{n+1}} \int_{y_{j-\frac{1}{2}}}^{y_{j+\frac{1}{2}}} \epsilon\theta\tilde{\beta}_x \tilde{I}_{i+\frac{1}{2},j,m} dy dt \\
&\triangleq F^1_{i+\frac{1}{2},j,m} + F^2_{i+\frac{1}{2},j,m}, \\
F_{i-\frac{1}{2},j,m} &= \int_{t^n}^{t^{n+1}} \int_{y_{j-\frac{1}{2}}}^{y_{j+\frac{1}{2}}} \mu_m I_{i-\frac{1}{2},j,m} dy dt + \int_{t^n}^{t^{n+1}} \int_{y_{j-\frac{1}{2}}}^{y_{j+\frac{1}{2}}} \epsilon\theta\tilde{\beta}_x \tilde{I}_{i-\frac{1}{2},j,m} dy dt \\
&\triangleq F^1_{i-\frac{1}{2},j,m} + F^2_{i-\frac{1}{2},j,m}, \\
G_{i,j+\frac{1}{2},m} &= \int_{t^n}^{t^{n+1}} \int_{x_{i-\frac{1}{2}}}^{x_{i+\frac{1}{2}}} \xi_m I_{i,j+\frac{1}{2},m} dx dt + \int_{t^n}^{t^{n+1}} \int_{x_{i-\frac{1}{2}}}^{x_{i+\frac{1}{2}}} \epsilon\theta\tilde{\beta}_y \tilde{I}_{i,j+\frac{1}{2},m} dx dt \\
&\triangleq G^1_{i,j+\frac{1}{2},m} + G^2_{i,j+\frac{1}{2},m}, \\
G_{i,j-\frac{1}{2},m} &= \int_{t^n}^{t^{n+1}} \int_{x_{i-\frac{1}{2}}}^{x_{i+\frac{1}{2}}} \xi_m I_{i,j-\frac{1}{2},m} dx dt + \int_{t^n}^{t^{n+1}} \int_{x_{i-\frac{1}{2}}}^{x_{i+\frac{1}{2}}} \epsilon\theta\tilde{\beta}_y \tilde{I}_{i,j-\frac{1}{2},m} dx dt \\
&\triangleq G^1_{i,j-\frac{1}{2},m} + G^2_{i,j-\frac{1}{2},m}, \\
S^{n+1}_{i,j,m} &= -\left(\tfrac{\sigma_t}{\epsilon}\right)^{n+1}_{i,j} I^{n+1}_{i,j,m} + \left(\tfrac{\sigma_t}{\epsilon} - \epsilon\sigma_s\right)^{n+1}_{i,j} \tfrac{1}{2\pi} ac(T^{n+1}_{i,j})^4 + \left(\tfrac{\epsilon\sigma_s}{2\pi}\right)^{n+1}_{i,j} c(E_r)^{n+1}_{i,j} \\
&\quad - \tfrac{1}{2\pi}(\sigma_t)^{n+1}_{i,j} \vec{\beta}^a_{i,j} \cdot \left[(\vec{F}_r)^{n+1}_{i,j} - \left(\tfrac{4}{3} - \theta\right)\epsilon(E_r)^{n+1}_{i,j} \vec{\tilde{v}}_{i,j}\right] \\
&\quad + \tfrac{3}{2\pi}\left(\tfrac{4}{3} - \theta\right)(\sigma_t)^{n+1}_{i,j}(E_r)^{n+1}_{i,j} \vec{\Omega} \cdot \vec{\tilde{v}}_{i,j}.
\end{aligned} \tag{3.13}$$

With $\vec{\beta} = (\beta_x, \beta_y)$ and $\vec{\beta}^a_{i,j} = (\vec{\beta}^{n+1}_{i,j} + \vec{\beta}^h_{i,j})/2$, $\vec{\tilde{v}}_{i,j} = \vec{v}^h_{i,j}$, the conservation of total momentum and total energy in (2.2) can be kept. The boundary values of $\tilde{I}$ in $F^2_{i\pm\frac{1}{2},j,m}$ and $G^2_{i,j\pm\frac{1}{2},m}$ are obtained explicitly through the upwinding according to the fluid velocity $\vec{\tilde{v}}$ on the boundary. In order to solve Eq. (3.12) completely, two key points have to be clarified. One is the determination of the boundary intensity I in (3.13) in order to evaluate the numerical boundary fluxes $F^1_{i\pm\frac{1}{2},j,m}$ and $G^1_{i,j\pm\frac{1}{2},m}$. Another one is to get the macroscopic variables T, E_r and $\vec{F}_r$ at time step t^{n+1} in order to discretize the source term $S^{n+1}_{i,j,m}$ implicitly.

For the cell interface radiation intensity, we now give the solution in the integral form of the radiative transfer equations at the boundary. Denote $\phi = acT^4$, around the center of a cell interface $\vec{x}_s = (x_{i-\frac{1}{2}}, y_j)$, the radiative transfer equation becomes

$$\begin{cases}
\frac{\epsilon}{c}\partial_t I_m + \mu_m \partial_x I_m + \epsilon\partial_x(\theta\tilde{\beta}_x\tilde{I}_m) = \left(\frac{\sigma_t}{\epsilon} - \epsilon\sigma_s\right)\frac{\tilde{\phi}}{2\pi} + \epsilon\sigma_s\frac{c\tilde{E}_r}{2\pi} - \frac{\sigma_t}{\epsilon} I_m + \bar{S}_m, \\
\bar{S}_m = -\frac{1}{2\pi}\sigma_t\vec{\beta}^a \cdot [\vec{F}_r - \left(\frac{4}{3} - \theta\right)\epsilon\bar{E}_r\vec{\tilde{v}}] + \frac{3}{2\pi}\left(\frac{4}{3} - \theta\right)\sigma_t\bar{E}_r\vec{\Omega}\cdot\vec{\tilde{v}}, \\
I_m(x, y_j, t)|_{t=t^n} = I_{m,0}(x, y_j).
\end{cases} \tag{3.14}$$

Here we should remark that the initial intensity $I_{m,0}$ and the functions $\tilde{\phi}$, $\tilde{E}_r$, $\vec{F}_r$ will be determined later.

Solving the above equations, the integral solution of (3.14) can be represented by

$$\begin{aligned}
I_m(t, x_{i-1/2}, y_j, \mu_m, \xi_m) &= \int_{t^n}^{t} \frac{c}{\epsilon} e^{-\sigma_{i-\frac{1}{2},j}(t-s)} (\bar{S}_m - \epsilon\partial_x(\theta\tilde{\beta}_x\tilde{I}_m)) ds \\
&+ e^{-\sigma_{i-1/2,j}(t-t^n)} I_{m,0}\Big(x_{i-1/2} - \frac{c\mu_m}{\epsilon}(t-t^n)\Big) \\
&+ \int_{t^n}^{t} \frac{c}{\epsilon} e^{-\sigma_{i-\frac{1}{2},j}(t-s)} \Big(\Big(\frac{\sigma_t}{\epsilon} - \epsilon\sigma_s\Big)\frac{\tilde{\phi}}{2\pi} + \epsilon\sigma_s\frac{c\tilde{E}_r}{2\pi}\Big)\Big(s, x_{i-1/2} - \frac{c\mu_m}{\epsilon}(t-s)\Big) ds,
\end{aligned} \tag{3.15}$$

where $\sigma = \frac{c\sigma_t}{\epsilon^2}$ and $\sigma_{i-1/2,j}$ is the value of σ at the corresponding cell interface. Moreover, in order to keep the asymptotic preserving property of the scheme, the values $\bar{E}_r$, $\vec{\tilde{v}}$, $\vec{\beta}^a$ in $\bar{S}_m$ should be consistently determined from those in the boundary flux $F^2_{i-\frac{1}{2},j,m}$, such as

$$\bar{E}_r = \int \tilde{I} d\vec{\Omega} = \sum_{i=1}^{M} \tilde{I}_m \omega_m, \quad \vec{\tilde{v}} = \vec{v}^h \ \text{ and } \ \vec{\beta}^a = \frac{1}{2}(\vec{v}^h + \vec{v}^{n+1}).$$

The derivative term $\epsilon \partial_x(\theta \tilde{\beta}_x \tilde{I}_m)$ is given by

$$\epsilon \partial_x(\theta \tilde{\beta}_x \tilde{I}_m) = \frac{\epsilon\theta((\tilde{\beta}_x \tilde{I}_m)|_{(i,j)} - (\tilde{\beta}_x \tilde{I}_m)|_{(i-1,j)})}{(\Delta x_i + \Delta x_{i-1})/2}.$$

For the determination of the boundary intensity I in (3.15) completely, the initial data $I_{m,0}$ is reconstructed by a piecewise polynomial

$$I_{m,0}(x, y_j) = \begin{cases} I^n_{i-1,j,m} + \delta_x I^n_{i-1,j,m}(x - x_{i-1,j}), & \text{if } x < x_{i-1/2,j}, \\ I^n_{i,j,m} + \delta_x I^n_{i,j}(x - x_{i,j}), & \text{if } x > x_{i-1/2,j}. \end{cases} \tag{3.16}$$

The two spatial derivatives $\delta_x I^n_{i,j}$ and $\delta_x I^n_{i-1,j,m}$ are the reconstructed slopes at cell centers of (i, j) and $(i-1, j)$ in the x-direction, respectively. In order to remove possible numerical oscillations, the MUSCL limiter [26] is used in (3.16).

The quantities $\tilde{\phi}$ and $\tilde{E}_r$ are reconstructed implicitly in time by piecewise polynomials. For the variable $\tilde{\phi}$, the reconstruction reads as

$$\begin{aligned} \tilde{\phi}(x, y_j, t) = {} & \phi^{n+1}_{i-1/2,j} + \delta_t \phi^{n+1}_{i-1/2,j}(t - t^{n+1}) \\ & + \begin{cases} \delta_x \phi^{n+1,L}_{i-1/2,j}(x - x_{i-1/2,j}), & \text{if } x < x_{i-1/2,j}, \\ \delta_x \phi^{n+1,R}_{i-1/2,j}(x - x_{i-1/2,j}), & \text{if } x > x_{i-1/2,j}, \end{cases} \end{aligned} \tag{3.17}$$

where $\delta_t \phi^{n+1}_{i-1/2,j} = (\phi^{n+1}_{i-1/2,j} - \phi^n_{i-1/2,j})/\Delta t$ is the time derivative, and the spatial derivatives are

$$\delta_x \phi^{n+1,L}_{i-1/2,j} = \frac{\phi^{n+1}_{i-1/2,j} - \phi^{n+1}_{i-1,j}}{\Delta x_{i-1}/2}, \quad \delta_x \phi^{n+1,R}_{i-1/2,j} = \frac{\phi^{n+1}_{i,j} - \phi^{n+1}_{i-1/2,j}}{\Delta x_i/2}.$$

The reconstruction for $\tilde{E}_r$ can be done similarly.

Finally, we need to evaluate the term $\bar{S}_m$ in the Eq. (3.15). In order to keep the asymptotic preserving property of the scheme, this term should be given consistently with the terms $F^2_{i\pm\frac{1}{2},j,m}$ and $G^2_{i,j\pm\frac{1}{2},m}$ in (3.13), where the upwind side cell center value is used by the sign of the fluid velocity $\vec{\tilde{v}}$ at the boundary, such as

$$F^2_{i-1/2,j,m} = \begin{cases} \theta v^h_{x,i-1,j} I^n_{m,i-1,j}, & \text{if } 0.5(v_{x,i-1,j} + v_{x,i,j}) \le 0, \\ \theta v^h_{x,i,j} I^n_{m,i,j}, & \text{if } 0.5(v_{x,i-1,j} + v_{x,i,j}) > 0, \end{cases} \tag{3.18}$$

and

$$\begin{aligned} \bar{S}_{m,i-1/2,j} = {} & -\frac{1}{2\pi} \vec{\beta}^a \cdot \sigma_t^{n+1} [\vec{F}_r^{n+1} - \left(\frac{4}{3} - \theta\right) \epsilon E_r^n \vec{\tilde{v}}]|_{i-1/2,j} \\ & + \begin{cases} \frac{3}{2\pi}\left(\frac{4}{3} - \theta\right) \sigma_t^{n+1} E_r^n \vec{\Omega} \cdot \vec{\tilde{v}}|_{i-1,j}, & \text{if } 0.5(v_{x,i-1,j} + v_{x,i,j}) \le 0, \\ \frac{3}{2\pi}\left(\frac{4}{3} - \theta\right) \sigma_t^{n+1} E_r^n \vec{\Omega} \cdot \vec{\tilde{v}}|_{i,j}, & \text{if } 0.5(v_{x,i-1,j} + v_{x,i,j}) > 0. \end{cases} \end{aligned} \tag{3.19}$$

Here the upper script n and $n+1$ are corresponding to the time steps, and the values of the first term in $\bar{S}_{m,i-1/2,j}$ is given by the average of the corresponding values in the cell $(i-1,j)$ and (i,j). Up to now, the formulation of the cell interface radiation intensity I for flux evaluation has been presented, but their final determination depends on the solution of the macroscopic variables $\phi^{n+1}_{i-1/2,j}, \phi^{n+1}_{i-1,j}, \phi^{n+1}_{i,j}$ and $(E_r)^{n+1}_{i-1/2,j}, (E_r)^{n+1}_{i-1,j}, (E_r)^{n+1}_{i,j}$. These unknowns in I and the other unknowns in the source term $S^{n+1}_{i,j,m}$ of (3.13) will be determined as shown in the next subsection.

3.2.2 Evaluation of the Macroscopic Variables

In this subsection we shall determine the macroscopic variables in the boundary fluxes and source term. Instead of solving the radiative transfer equations, we first get the radiation energy transport equation by taking moments of the last equation in (2.1), and solve them together with the fluid dynamic equations:

$$\begin{cases} \partial_t(\rho\vec{v}) = -\frac{1}{c}\{-\frac{\sigma_t}{\epsilon}\vec{F}_r + \left(\frac{4}{3}-\theta\right)\sigma_t E_r\vec{v}\}, \\ \partial_t(\rho E) = -\frac{1}{\epsilon}\{(\frac{\sigma_t}{\epsilon}-\epsilon\sigma_s)(acT^4-cE_r) - \sigma_t\vec{\beta}\cdot[\vec{F}_r - \left(\frac{4}{3}-\theta\right)\epsilon E_r\vec{v}]\}, \\ \epsilon\dfrac{\partial E_r}{\partial t} + \langle\vec{\Omega}\cdot\nabla I\rangle + \epsilon\nabla\cdot\langle\theta\vec{\beta}I\rangle = (\dfrac{\sigma_t}{\epsilon}-\epsilon\sigma_s)(acT^4-cE_r) \\ \quad -\sigma_t\vec{\beta}\cdot[\vec{F}_r - \left(\frac{4}{3}-\theta\right)\epsilon E_r\vec{v}], \\ \dfrac{\epsilon}{c^2}\dfrac{\partial\vec{F}_r}{\partial t} + \dfrac{1}{c}\langle\vec{\Omega}\otimes\vec{\Omega}\cdot\nabla I\rangle + \dfrac{\epsilon}{c}\nabla\cdot\langle\theta\vec{\beta}\otimes\vec{\Omega}I\rangle = -\dfrac{\sigma_t}{c\epsilon}\vec{F}_r \\ \quad +\frac{1}{c}\left(\frac{4}{3}-\theta\right)\sigma_t E_r\vec{v}, \end{cases} \tag{3.20}$$

where the angular integrations are

$$\langle\vec{\Omega}\cdot\nabla I\rangle := \int\vec{\Omega}\nabla I d\vec{\Omega}, \quad \langle\vec{\Omega}\otimes\vec{\Omega}\cdot\nabla I\rangle := \int\vec{\Omega}\otimes\vec{\Omega}\nabla I d\vec{\Omega};$$
$$\langle\theta\vec{\beta}I\rangle := \int\theta\vec{\beta}I d\vec{\Omega}, \quad \langle\theta\vec{\beta}\otimes\vec{\Omega}I\rangle := \int\theta\vec{\beta}\otimes\vec{\Omega}I d\vec{\Omega}.$$

The finite volume method for system (3.20) reads as follows.

$$\begin{cases} \rho^{n+1}_{i,j}\vec{v}^{n+1}_{i,j} = \rho^{n+1}_{i,j}\vec{v}^{h}_{i,j} - \frac{\Delta t}{c}\{-\frac{\sigma^{n+1}_{t,i,j}}{\epsilon}(\vec{F}_r)^{n+1}_{i,j} + \left(\frac{4}{3}-\theta\right)\sigma^{n+1}_{t,i,j}(E_r)^{n+1}_{i,j}\vec{v}^{h}_{i,j}\}, \\ \rho^{n+1}_{i,j}E^{n+1}_{i,j} = \rho^{n+1}_{i,j}E^{h}_{i,j} - \frac{\Delta t}{\epsilon}\{(\frac{\sigma^{n+1}_{t,i,j}}{\epsilon}-\epsilon\sigma^{n+1}_{s,i,j})(ac(T^{n+1}_{i,j})^4 - c(E_r)^{n+1}_{i,j}) \\ - \quad \sigma^{n+1}_{t,i,j}\vec{\beta}^{a}_{i,j}\cdot[(\vec{F}_r)^{n+1}_{i,j} - \left(\frac{4}{3}-\theta\right)\epsilon(E_r)^{n+1}_{i,j}\vec{v}^{h}_{i,j}]\}, \\ \epsilon(E_r)^{n+1}_{i,j} + \dfrac{\Delta t}{\Delta x_i\Delta y_j}(\Phi^{n+1}_{i+\frac{1}{2},j} - \Phi^{n+1}_{i-\frac{1}{2},j}) + \dfrac{\Delta t}{\Delta x_i\Delta y_j}(\Psi^{n+1}_{i,j+\frac{1}{2}} - \Psi^{n+1}_{i,j-\frac{1}{2}}) \\ = \epsilon(E_r)^{n}_{i,j} + \Delta t\{(\frac{\sigma^{n+1}_{t,i,j}}{\epsilon}-\epsilon\sigma^{n+1}_{s,i,j})(ac(T^{n+1}_{i,j})^4 - c(E_r)^{n+1}_{i,j}) \\ - \quad \sigma^{n+1}_{t,i,j}\vec{\beta}^{a}_{i,j}\cdot[(\vec{F}_r)^{n+1}_{i,j} - \left(\frac{4}{3}-\theta\right)\epsilon(E_r)^{n+1}_{i,j}\vec{v}^{h}_{i,j}]\}, \\ \dfrac{\epsilon}{c^2}(\vec{F}_r)^{n+1}_{i,j} + \dfrac{\Delta t}{\Delta x_i\Delta y_j}(\vec{\Phi}^{n+1}_{i+\frac{1}{2},j} - \vec{\Phi}^{n+1}_{i-\frac{1}{2},j}) + \dfrac{\Delta t}{\Delta x_i\Delta y_j}(\vec{\Psi}^{n+1}_{i,j+\frac{1}{2}} - \vec{\Psi}^{n+1}_{i,j-\frac{1}{2}}) \\ = \dfrac{\epsilon}{c^2}(\vec{F}_r)^{n}_{i,j} + \Delta t\left\{-\dfrac{\sigma^{n+1}_{t,i,j}}{c\epsilon}(\vec{F}_r)^{n+1}_{i,j} + \dfrac{1}{c}\left(\dfrac{4}{3}-\theta\right)\sigma^{n+1}_{t,i,j}(E_r)^{n+1}_{i,j}\vec{v}^{h}_{i,j}\right\}, \end{cases} \tag{3.21}$$

where $\vec{\beta}^{a}_{i,j} = (\vec{\beta}^{n+1}_{i,j} + \vec{\beta}^{h}_{i,j})/2$.

It should be emphasized that the central ingredient in UGKS is about the use of the same time evolution distribution function for the microscopic and macroscopic fluxes at a cell interface [28]. Based on this methodology, the boundary fluxes in (3.21) are obtained by angular integration of F and G in (3.13),

$$\begin{aligned}
\Phi^{n+1}_{i+\frac{1}{2},j} &= \sum_{m=1}^{M} F_{i+\frac{1}{2},j,m}\omega_m = \sum_{m=1}^{M}\left(F^1_{i+\frac{1}{2},j,m} + F^2_{i+\frac{1}{2},j,m}\right)\omega_m,\\
\Phi^{n+1}_{i-\frac{1}{2},j} &= \sum_{m=1}^{M} F_{i-\frac{1}{2},j,m}\omega_m = \sum_{m=1}^{M}\left(F^1_{i-\frac{1}{2},j,m} + F^2_{i-\frac{1}{2},j,m}\right)\omega_m,\\
\Psi^{n+1}_{i,j+\frac{1}{2}} &= \sum_{m=1}^{M} G_{i,j+\frac{1}{2},m}\omega_m = \sum_{m=1}^{M}\left(G^1_{i,j+\frac{1}{2},m} + G^2_{i,j+\frac{1}{2},m}\right)\omega_m,\\
\Psi^{n+1}_{i,j-\frac{1}{2}} &= \sum_{m=1}^{M} G_{i,j-\frac{1}{2},m}\omega_m = \sum_{m=1}^{M}\left(G^1_{i,j-\frac{1}{2},m} + G^2_{i,j-\frac{1}{2},m}\right)\omega_m,\\
\vec{\Phi}^{n+1}_{i+\frac{1}{2},j} &= \frac{1}{c}\sum_{m=1}^{M} \vec{\Omega}_m F_{i+\frac{1}{2},j,m}\omega_m = \frac{1}{c}\sum_{m=1}^{M} \vec{\Omega}_m\left(F^1_{i+\frac{1}{2},j,m} + F^2_{i+\frac{1}{2},j,m}\right)\omega_m,\\
\vec{\Phi}^{n+1}_{i-\frac{1}{2},j} &= \frac{1}{c}\sum_{m=1}^{M} \vec{\Omega}_m F_{i-\frac{1}{2},j,m}\omega_m = \frac{1}{c}\sum_{m=1}^{M} \vec{\Omega}_m\left(F^1_{i-\frac{1}{2},j,m} + F^2_{i-\frac{1}{2},j,m}\right)\omega_m,\\
\vec{\Psi}^{n+1}_{i,j+\frac{1}{2}} &= \frac{1}{c}\sum_{m=1}^{M} \vec{\Omega}_m G_{i,j+\frac{1}{2},m}\omega_m = \frac{1}{c}\sum_{m=1}^{M} \vec{\Omega}_m\left(G^1_{i,j+\frac{1}{2},m} + G^2_{i,j+\frac{1}{2},m}\right)\omega_m,\\
\vec{\Psi}^{n+1}_{i,j-\frac{1}{2}} &= \frac{1}{c}\sum_{m=1}^{M} \vec{\Omega}_m G_{i,j-\frac{1}{2},m}\omega_m = \frac{1}{c}\sum_{m=1}^{M} \vec{\Omega}_m\left(G^1_{i,j-\frac{1}{2},m} + G^2_{i,j-\frac{1}{2},m}\right)\omega_m.
\end{aligned} \tag{3.22}$$

Thus, based on the macroscopic interface fluxes in (3.22), the system (3.21) reduces to a coupled nonlinear system of the macroscopic quantities $\vec{v}^{n+1}_{i,j}$, $T^{n+1}_{i,j}$, $(E_r)^{n+1}_{i,j}$ and $(\vec{F}_r)^{n+1}_{i,j}$ only, where the parameters $\sigma^{n+1}_{t,i,j}$ and $\sigma^{n+1}_{s,i,j}$ depend implicitly on the material temperature $T^{n+1}_{i,j}$. This nonlinear system can be solved by iterative method, such as the Gauss-Seidel iteration method as shown in [11,12].

3.2.3 Update of the Solution

After obtaining the macroscopic variables $T^{n+1}_{i,j}$, $(E_r)^{n+1}_{i,j}$ and $(\vec{F}_r)^{n+1}_{i,j}$ by solving the Eq. (3.21) iteratively, we can fully determine the radiation intensity at the cell interface for the microscopic flux evaluation. For example, the boundary value $\phi^{n+1}_{i-\frac{1}{2},j}$ in (3.17) is given by

$$\phi^{n+1}_{i,j-1/2} = (\phi^{n+1}_{i,j} + \phi^{n+1}_{i,j-1})/2.$$

The left and right derivatives in (3.17) are given by

$$\delta_x\phi^{n+1,L}_{i-1/2,j} = \frac{\phi^{n+1}_{i-1/2,j} - \phi^{n+1}_{i-1,j}}{\Delta x_{i-1}/2}, \quad \delta_x\phi^{n+1,R}_{i,j-1/2} = \frac{\phi^{n+1}_{i,j} - \phi^{n+1}_{i-1/2,j}}{\Delta x_i/2}.$$

For the time derivative $\delta_t\phi^{n+1}_{i-1/2,j}$ in (3.17), we can take

$$\delta_t\phi^{n+1}_{i-1/2,j} = \frac{\phi^{n+1}_{i-1/2,j} - \phi^{n}_{i-1/2,j}}{\Delta t}.$$

In the same way, the reconstruction of $\tilde{E}_r$ in (3.15) can be obtained.

With the determined macroscopic variables in (3.21), the source term $S_{i,j,m}^{n+1}$ and the numerical boundary fluxes $F_{i\pm\frac{1}{2},j,m}$, $G_{i,j\pm\frac{1}{2},m}$ in (3.13) can be evaluated explicitly. Afterwards, the radiative intensity in (3.12) can be updated as follows.

$$\begin{cases} \hat{S}_{i,j,m}^{n+1} \triangleq \left(\frac{\sigma_t}{\epsilon} - \epsilon\sigma_s\right)_{i,j}^{n+1} \frac{1}{2\pi} ac(T_{i,j}^{n+1})^4 + \left(\frac{\epsilon\sigma_s}{2\pi}\right)_{i,j}^{n+1} c(E_r)_{i,j}^{n+1} \\ \quad -\frac{1}{2\pi}(\sigma_t)_{i,j}^{n+1} \vec{\beta}_{i,j}^{a} \cdot \left[(\vec{F}_r)_{i,j}^{n+1} - \left(\frac{4}{3} - \theta\right)\epsilon(E_r)_{i,j}^{n+1}\vec{\tilde{v}}_{i,j}\right] \\ \quad +\frac{3}{2\pi}\left(\frac{4}{3} - \theta\right)(\sigma_t)_{i,j}^{n+1}(E_r)_{i,j}^{n+1}\vec{\Omega}\cdot\vec{\tilde{v}}_{i,j}, \\ I_{i,j}^{n+1} = \dfrac{\frac{\epsilon}{c\Delta t} I_{i,j}^{n} + \frac{F_{i-\frac{1}{2},j,m} - F_{i+\frac{1}{2},j,m}}{\Delta x_i \Delta y_j} + \frac{G_{i,j-\frac{1}{2},m} - G_{i,j+\frac{1}{2},m}}{\Delta x_i \Delta y_j} + \hat{S}_{i,j,m}^{n+1}}{\frac{\epsilon}{c\Delta t} + \left(\frac{\sigma_t}{c}\right)_{i,j}^{n+1}}. \end{cases} \tag{3.23}$$

This completes the main numerical procedures in our unified gas kinetic scheme.

The final step is to update the solutions in the first and second equations in (3.12) for the fluid velocity $\vec{v}_{i,j}^{n+1}$ and material temperature $\hat{T}_{i,j}^{n+1}$ with the newly obtained value $I_{i,j,m}^{n+1}$. The solutions for the momentum equation (3.12) and the energy equation (3.12) are given respectively by

$$\begin{cases} \vec{v}_{i,j}^{n+1} = \dfrac{\rho_{i,j}^{n+1}\vec{v}_{i,j}^{h} - \frac{\Delta t}{c}\sum_{m=1}^{M}\vec{\Omega}_m(\hat{S}_{i,j,m}^{n+1} + (\frac{\sigma_t}{c})_{i,j}^{n+1} I_{i,j,m}^{n+1})\omega_m}{\rho_{i,j}^{n+1}}, \\ \hat{E}_{i,j}^{n+1} = \dfrac{\rho_{i,j}^{n+1}E_{i,j}^{h} - \frac{\Delta t}{\epsilon}\sum_{m=1}^{M}(\hat{S}_{i,j,m}^{n+1} + (\frac{\sigma_t}{c})_{i,j}^{n+1} I_{i,j,m}^{n+1})\omega_m}{\rho_{i,j}^{n+1}}, \\ \hat{T}_{i,j}^{n+1} = \dfrac{\hat{E}_{i,j}^{n+1} - |\vec{v}_{i,j}^{n+1}|^2/2}{C_v}. \end{cases} \tag{3.24}$$

Based on (3.23) and (3.24), we get the solution of the system (3.10), and complete the construction of the GKS and UGKS algorithm for the radiation hydrodynamic system.

Here we summarize the whole solving procedure of the GKS-UGKS algorithm for the radiation hydrodynamic system:

Loop of the GKS-UGKS for the radiation hydrodynamics (2.1) Given $\rho_{i,j}^{n}$, $\vec{v}_{i,j}^{n}$, $I_{i,j,m}^{n}$ and $T_{i,j}^{n}$, one has $(E_r)_{i,j}^{n}$, $(\vec{F}_r)_{i,j}^{n}$ and $\phi_{i,j}^{n}$. Find $\rho_{i,j}^{n+1}$, $\vec{v}_{i,j}^{n+1}$, $I_{i,j,m}^{n+1}$ and $\hat{T}_{i,j}^{n+1}$.

(1) Solve the hydrodynamics equation (3.1) by GKS method to to get $\rho_{i,j}^{n+1}$, $\vec{v}_{i,j}^{h}$ and the intermediate total material energy $E_{i,j}^{h}$;

(2) Solve the nonlinear system (3.21) to get $\vec{v}_{i,j}^{n+1}$, $E_{i,j}^{n+1}$, $(E_r)_{i,j}^{n+1}$, $(\vec{F}_r)_{i,j}^{n+1}$;

(3) With the auxiliary macro quantities in step 2, construct the numerical boundary fluxes in (3.13) with the boundary intensity given by (3.15). Then solve the Eq. (3.23) to obtain $I_{i,j,m}^{n+1}$.

(4) Using the newly updated $I_{i,j,m}^{n+1}$ obtained in step 3, solve the Eq. (3.24) to get the final $\vec{v}_{i,j}^{n+1}$, $\hat{T}_{i,j}^{n+1}$.

(5) Setting $\rho_{i,j}^{n} = \rho_{i,j}^{n+1}$, $\vec{v}_{i,j}^{n} = \vec{v}_{i,j}^{n+1}$, $I_{i,j,m}^{n} = I_{i,j,m}^{n+1}$, $T_{i,j}^{n} = \hat{T}_{i,j}^{n+1}$, and goto step 1 for the next computational time step.

End

In the following section, the asymptotic preserving property of the proposed scheme will be analyzed.

4 Asymptotic Analysis of the Scheme

The scheme presented in the last section possesses the asymptotic preserving (AP) property. In fact, following the analysis in [11,12], we are able to show such a property for the scheme in capturing the diffusion solution in the optically thick region for the radiative transfer. The numerical fluxes F and G in (3.13) play a dominant role in the proof of the AP property. Firstly, the left boundary numerical flux in the x-direction is given by

$$\frac{c}{\epsilon}F^1_{i,j-1/2,m} = \frac{c\mu_m\Delta y_j}{\epsilon\Delta t}\int_{t^n}^{t^{n+1}} I_m(t, x_{i-1/2}, y_j, \mu_m, \xi_m)dt,$$

which can be exactly evaluated as follows. For simplicity, with the notation $\varphi = cE_r$,, based on (3.15), the above integral can be obtained

$$\begin{aligned}
\tfrac{c}{\epsilon}F^1_{i-1/2,j,m} = \Delta y_j\{&A_{i-1/2,j}\mu_m(I^{n,-}_{i-1/2,j,m}1_{\mu_m>0} + I^{n,+}_{i-1/2,j,m}1_{\mu_m<0})\\
&+ D^1_{i-1/2,j}(\mu_m^2\delta_x\phi^{n+1,L}_{i-1/2,j}1_{\mu_m>0} + \mu_m^2\delta_x\phi^{n+1,R}_{i-1/2,j}1_{\mu_m<0})\\
&+ D^2_{i-1/2,j}(\mu_m^2\delta_x\varphi^{n+1,L}_{i-1/2,j}1_{\mu_m>0} + \mu_m^2\delta_x\varphi^{n+1,R}_{i-1/2,j}1_{\mu_m<0})\\
&+ B_{i-1/2,j}(\mu_m^2\delta_x I^n_{i-1,j,m}1_{\mu_m>0} + \mu_m^2\delta_x I^n_{i,j,m}1_{\mu_m<0})\\
&+ E^1_{i-1/2,j}\mu_m\delta_t\phi^{n+1}_{i-1/2,j} + C^1_{i-1/2,j}\mu_m\phi^{n+1}_{i-1/2,j}\\
&+ E^2_{i-1/2,j}\mu_m\delta_t\varphi^{n+1}_{i-1/2,j} + C^2_{i-1/2,j}\mu_m\varphi^{n+1}_{i-1/2,j}\\
+P_{i-1/2,j}\mu_m(\bar{S}_m - \epsilon\partial_x(\theta\tilde{\beta}_x\tilde{I}_m))|_{i-\frac{1}{2},j}\}.&
\end{aligned} \tag{4.1}$$

Here $I^{n,-}_{i-1/2,j,m}$, $I^{n,+}_{i-1/2,j,m}$ are the interface values given by

$$\begin{aligned}
I^{n,-}_{i-1/2,j,m} &= I^n_{i-1,j,m} + \delta_x I^n_{i-1,j,m}(x_{i-1/2} - x_{i-1,j}),\\
I^{n,+}_{i-1/2,j,m} &= I^n_{i,j,m} + \delta_x I^n_{i,j,m}(x_{i-1/2} - x_{i,j}),
\end{aligned}$$

and $\delta_x I^n_{i-1,j,m}$ and $\delta_x I^n_{i,j,m}$ are slopes in the x-direction which are reconstructed in (3.16). The coefficients in (4.1) are given by

$$\begin{aligned}
A &= \tfrac{c}{\epsilon\Delta t\nu}(1-e^{-\nu\Delta t}),\\
C^1 &= \tfrac{c^2(\frac{\sigma_t}{\epsilon}-\epsilon\sigma_s)}{2\pi\Delta t\epsilon^2\nu}(\Delta t - \tfrac{1}{\nu}(1-e^{-\nu\Delta t})),\\
C^2 &= \tfrac{c^2\epsilon\sigma_s}{2\pi\Delta t\epsilon^2\nu}(\Delta t - \tfrac{1}{\nu}(1-e^{-\nu\Delta t})),\\
D^1 &= -\tfrac{c^3(\frac{\sigma_t}{\epsilon}-\epsilon\sigma_s)}{2\pi\Delta t\epsilon^3\nu^2}(\Delta t(1+e^{-\nu\Delta t}) - \tfrac{2}{\nu}(1-e^{-\nu\Delta t})),\\
D^2 &= -\tfrac{c^3\epsilon\sigma_s}{2\pi\Delta t\epsilon^3\nu^2}(\Delta t(1+e^{-\nu\Delta t}) - \tfrac{2}{\nu}(1-e^{-\nu\Delta t})),\\
B &= -\tfrac{c^2}{\epsilon^2\nu^2\Delta t}(1-e^{-\nu\Delta t} - \nu\Delta t e^{-\nu\Delta t}),\\
E^1 &= \tfrac{c^2(\frac{\sigma_t}{\epsilon}-\epsilon\sigma_s)}{2\pi\epsilon^2\nu^3\Delta t}(1-e^{-\nu\Delta t} - \nu\Delta t e^{-\nu\Delta t} - \tfrac{1}{2}(\nu\Delta t)^2),\\
E^2 &= \tfrac{c^2\epsilon\sigma_s}{2\pi\epsilon^2\nu^3\Delta t}(1-e^{-\nu\Delta t} - \nu\Delta t e^{-\nu\Delta t} - \tfrac{1}{2}(\nu\Delta t)^2),\\
P &= \tfrac{c^2}{\Delta t\epsilon^2\nu}(\Delta t - \tfrac{1}{\nu}(1-e^{-\nu\Delta t}))
\end{aligned} \tag{4.2}$$

with $\nu = \frac{c\sigma_t}{\epsilon^2}$.

The behavior of the scheme in the small-ϵ limit is completely controlled by the limits of these coefficients, as shown in the following proposition.

Proposition 1 *Let σ_t and σ_s be positive. Then, as ϵ tends to zero, we have*

- $A(\Delta t, \epsilon, \sigma, \nu) \to 0$;
- $B(\Delta t, \epsilon, \sigma, \nu) \to 0$;
- $D^1(\Delta t, \epsilon, \sigma, \nu) \to -c/(2\pi\sigma_t)$;
- $D^2(\Delta t, \epsilon, \sigma, \nu) \to 0$;
- $P(\Delta t, \epsilon, \sigma, \nu) \to c/\sigma_t$;
- $\frac{\epsilon}{c^2} E^1(\Delta t, \epsilon, \sigma, \nu) \to -\Delta t/(4\pi c)$;
- $\frac{\epsilon}{c^2} E^2(\Delta t, \epsilon, \sigma, \nu) \to 0$;
- $\frac{\epsilon}{c^2} C^1(\Delta t, \epsilon, \sigma, \nu) \to 1/(2\pi c)$;
- $\frac{\epsilon}{c^2} C^2(\Delta t, \epsilon, \sigma, \nu) \to 0$.

Taking moment of the left boundary flux $F_{i-\frac{1}{2},j,m}$ over the propagation angle $\vec{\Omega}$, we obtain

$$
\begin{aligned}
\frac{c}{\epsilon}\Phi^{n+1}_{i-\frac{1}{2},j} &= \frac{c}{\epsilon}\sum_{m=1}^{M} F_{i-\frac{1}{2},j,m}\omega_m = \frac{c}{\epsilon}\sum_{m=1}^{M}(F^1_{i-\frac{1}{2},j,m} + F^2_{i-\frac{1}{2},j,m})\omega_m \\
&= \Delta y_j \left\{ A_{i-1/2,j}\sum_{m=1}^{M}\omega_m\mu_m\left(I^n_{i-1,j,m}1_{\mu_m>0} + I^n_{i,j,m}1_{\mu_m<0}\right)\right. \\
&\quad + \frac{2\pi D^1_{i-1/2,j}}{3}\left(\frac{\phi^{n+1}_{i,j} - \phi^{n+1}_{i-1,j}}{0.5(\Delta x_i + \Delta x_{i-1})}\right) + \frac{2\pi D^2_{i-1/2,j}}{3}\left(\frac{\varphi^{n+1}_{i,j} - \varphi^{n+1}_{i-1,j}}{0.5(\Delta x_i + \Delta x_{i-1})}\right) \\
&\quad + \left(\frac{4}{3} - \theta\right)c\bar{E}_r\tilde{v}_x|_{i-\frac{1}{2},j} - \frac{c}{\sigma_t}\sum_{m=1}^{M}\omega_m\mu_m(\epsilon\partial_x(\theta\tilde{\beta}_x\tilde{I}_m))|_{i-\frac{1}{2},j} \\
&\quad \left. + B_{i-1/2,j}\sum_{m=1}^{M}\omega_m\mu_m^2(\delta_x I^n_{i-1,j,m}1_{\mu_m>0} + \delta_x I^n_{i,j,m}1_{\mu_m<0}) + \theta c\bar{E}_r\tilde{v}_x|_{i-\frac{1}{2},j}\right\} \qquad (4.3) \\
&= \Delta y_j \left\{ A_{i-1/2,j}\sum_{m=1}^{M}\omega_m\mu_m\left(I^n_{i-1,j,m}1_{\mu_m>0} + I^n_{i,j,m}1_{\mu_m<0}\right)\right. \\
&\quad + \frac{2\pi D^1_{i-1/2,j}}{3}\left(\frac{\phi^{n+1}_{i,j} - \phi^{n+1}_{i-1,j}}{0.5(\Delta x_i + \Delta x_{i-1})}\right) + \frac{2\pi D^2_{i-1/2,j}}{3}\left(\frac{\varphi^{n+1}_{i,j} - \varphi^{n+1}_{i-1,j}}{0.5(\Delta x_i + \Delta x_{i-1})}\right) \\
&\quad + \frac{4}{3}c\bar{E}_r\tilde{v}_x|_{i-\frac{1}{2},j} - \frac{c\epsilon}{\sigma_t}\sum_{m=1}^{M}\omega_m\mu_m(\partial_x(\theta\tilde{\beta}_x\tilde{I}_m))|_{i-\frac{1}{2},j} \\
&\quad \left. + B_{i-1/2,j}\sum_{m=1}^{M}\omega_m\mu_m^2(\delta_x I^n_{i-1,j,m}1_{\mu_m>0} + \delta_x I^n_{i,j,m}1_{\mu_m<0})\right\} \\
&\quad \xrightarrow[\epsilon\to 0]{} \Delta y_j\left\{-\frac{c}{3\sigma_t}\frac{\phi^{n+1}_{i,j} - \phi^{n+1}_{i-1,j}}{0.5(\Delta x_i + \Delta x_{i-1})} + \frac{4}{3}c(\bar{E}_r\tilde{v}_x)|_{i-\frac{1}{2},j}\right\},
\end{aligned}
$$

and

$$\begin{aligned}
\vec{\bar{\Phi}}^{n+1}_{i-\frac{1}{2},j} &= \frac{1}{c}\sum_{m=1}^{M}\vec{\Omega}_m F_{i-\frac{1}{2},j,m}\omega_m = \frac{1}{c}\sum_{m=1}^{M}\vec{\Omega}_m (F^1_{i-\frac{1}{2},j,m} + F^2_{i-\frac{1}{2},j,m})\omega_m \\
&= \frac{\epsilon}{c^2}\Delta y_j \sum_{m=1}^{M}\vec{\Omega}_m \{A_{i-1/2,j}\mu_m (I^{n,-}_{i-1/2,j,m}1_{\mu_m>0} + I^{n,+}_{i-1/2,j,m}1_{\mu_m<0}) \\
&\quad + D^1_{i-1/2,j}(\mu_m^2\delta_x\phi^{n+1,L}_{i-1/2,j}1_{\mu_m>0} + \mu_m^2\delta_x\phi^{n+1,R}_{i-1/2,j}1_{\mu_m<0}) \\
&\quad + D^2_{i-1/2,j}(\mu_m^2\delta_x\varphi^{n+1,L}_{i-1/2,j}1_{\mu_m>0} + \mu_m^2\delta_x\varphi^{n+1,R}_{i-1/2,j}1_{\mu_m<0}) \\
&\quad + B_{i-1/2,j}(\mu_m^2\delta_x I^n_{i-1,j,m}1_{\mu_m>0} + \mu_m^2\delta_x I^n_{i,j,m}1_{\mu_m<0}) \\
&\quad + E^1_{i-1/2,j}\mu_m\delta_t\phi^{n+1}_{i-1/2,j} + C^1_{i-1/2,j}\mu_m\phi^{n+1}_{i-1/2,j} \\
&\quad + E^2_{i-1/2,j}\mu_m\delta_t\varphi^{n+1}_{i-1/2,j} + C^2_{i-1/2,j}\mu_m\varphi^{n+1}_{i-1/2,j} \\
&\quad + P_{i-1/2,j}\mu_m(\bar{S}_m - \epsilon\partial_x(\theta\tilde{\beta}_x\tilde{I}_m))|_{i-\frac{1}{2},j}\}\omega_m \\
&\xrightarrow[\epsilon\to 0]{} \Delta y_j\sum_{m=1}^{M}\vec{\Omega}_m\{\frac{1}{2\pi c}\mu_m\phi^{n+1}_{i-1/2,j} - \frac{\Delta t}{4\pi c}\mu_m\delta_t\phi^{n+1}_{i-1/2,j}\}\omega_m \\
&= \frac{\Delta y_j}{3c}(\phi^{n+1}_{i-1/2,j} - \frac{\Delta t}{2}\delta_t\phi^{n+1}_{i-1/2,j})\vec{e}_1^{\,T} = \frac{\Delta y_j}{3c}\frac{\phi^{n+1}_{i-1/2,j} + \phi^{n}_{i-1/2,j}}{2}\vec{e}_1^{\,T}.
\end{aligned} \tag{4.4}$$

With $\vec{e}_1 = (1, 0)$ is the unit vector, then by the limits in (4.3) and (4.5), it is easy to see that the above coupled GKS and UGKS method possesses the asymptotic preserving property, provided the following proposition holds.

Proposition 2 *Let σ_t and σ_s be positive. Then, as ϵ tends to zero, the numerical scheme given by coupling (3.6) for the fluid and (3.12) for the radiation goes to the standard implicit central difference scheme for the equilibrium diffusion limit system (2.9) of radiation hydrodynamics.*

Proof Firstly, as $\epsilon \to 0$, the term of ϵ^{-1}-order in the third equation of (3.12) satisfies

$$I^{n+1}_{i,j,m} \to \frac{1}{2\pi}\phi^{n+1}_{i,j} = \frac{1}{2\pi}ac(T^{n+1}_{i,j})^4. \tag{4.5}$$

Integrating the above equation with respect to the angular variable, we find that

$$c(E_r)^{n+1}_{i,j} \to \phi^{n+1}_{i,j} = ac(T^{n+1}_{i,j})^4, \quad (\vec{F}_r)^{n+1}_{i,j} \to 0, \quad \bar{\bar{P}}^{n+1}_{i,j} \to \frac{1}{3}a(T^{n+1}_{i,j})^4\bar{\bar{D}}. \tag{4.6}$$

Secondly, we integrate the flux $\frac{1}{\epsilon}F^{k+1}_{i-1/2,j}$ in the angular variable to obtain the macro flux $\frac{1}{\epsilon}\Phi^{k+1}_{i-1/2,j,m,n}$ in (4.5). Then, taking $\epsilon \to 0$, under Proposition 1 we obtain

$$\frac{1}{\epsilon}\Phi^{n+1}_{i-1/2,j} \to \Delta y_j\Big(-\frac{1}{3\sigma^{n+1}_{i-1/2,j}}\frac{\phi^{n+1}_{i,j} - \phi^{n+1}_{i-1,j}}{0.5*(\Delta x_i + \Delta x_{i-1})} + \frac{4}{3}(\bar{E}_r\tilde{v}_x)|_{i-\frac{1}{2},j}\Big). \tag{4.7}$$

Similarly, as $\epsilon \to 0$, the other macro boundary interface fluxes go to

$$\begin{aligned}
\tfrac{1}{\epsilon}\Phi^{n+1}_{i+1/2,j} &\to \Delta y_j\Big(-\frac{1}{3\sigma^{n+1}_{i+1/2,j}}\frac{\phi^{n+1}_{i+1,j}-\phi^{n+1}_{i,j}}{0.5*(\Delta x_i+\Delta x_{i+1})}+\frac{4}{3}(\bar{E}_r\tilde{v}_x)|_{i+\frac{1}{2},j}\Big),\\
\tfrac{1}{\epsilon}\Psi^{n+1}_{i,j-1/2} &\to \Delta x_i\Big(-\frac{1}{3\sigma^{n+1}_{i,j-1/2}}\frac{\phi^{n+1}_{i,j}-\phi^{n+1}_{i,j-1}}{0.5*(\Delta y_j+\Delta y_{j-1})}+\frac{4}{3}(\bar{E}_r\tilde{v}_y)|_{i,j-\frac{1}{2}}\Big),\\
\tfrac{1}{\epsilon}\Psi^{n+1}_{i,j+1/2} &\to \Delta x_i\Big(-\frac{1}{3\sigma^{n+1}_{i,j+1/2}}\frac{\phi^{n+1}_{i,j+1}-\phi^{n+1}_{i,j}}{0.5*(\Delta y_j+\Delta y_{j+1})}+\frac{4}{3}(\bar{E}_r\tilde{v}_y)|_{i,j+\frac{1}{2}}\Big).
\end{aligned} \tag{4.8}$$

Dividing the third equation of (3.12) by ϵ and integrating the resulting equation over the angular variable, with the utilization of second equation of (3.12) and Eq.(4.8), as $\epsilon \to 0$ the energy transport equation goes to

$$\begin{aligned}
&\rho^{n+1}_{i,j}\frac{E^{n+1}_{i,j}-E^{n}_{i,j}}{\Delta t}+\frac{(E_r)^{n+1}_{i,j}-(E_r)^{n}_{i,j}}{\Delta t}\\
&+\frac{1}{\Delta x_i}\left\{\left(-\frac{1}{3\sigma^{n+1}_{i+1/2,j}}\frac{\phi^{n+1}_{i+1,j}-\phi^{n+1}_{i,j}}{0.5*(\Delta x_i+\Delta x_{i+1})}+\frac{4}{3}(\bar{E}_r\tilde{v}_x)|_{i+\frac{1}{2},j}\right)\right.\\
&\left.-\left(-\frac{1}{3\sigma^{n+1}_{i-1/2,j}}\frac{\phi^{n+1}_{i,j}-\phi^{n+1}_{i-1,j}}{0.5*(\Delta x_i+\Delta x_{i-1})}+\frac{4}{3}(\bar{E}_r\tilde{v}_x)|_{i-\frac{1}{2},j}\right)\right\}\\
&+\frac{1}{\Delta y_j}\left\{\left(-\frac{1}{3\sigma^{n+1}_{i,j+1/2}}\frac{\phi^{n+1}_{i,j+1}-\phi^{n+1}_{i,j}}{0.5*(\Delta y_j+\Delta y_{j+1})}+\frac{4}{3}(\bar{E}_r\tilde{v}_y)|_{i,j+\frac{1}{2}}\right)\right.\\
&\left.-\left(-\frac{1}{3\sigma^{n+1}_{i,j-1/2}}\frac{\phi^{n+1}_{i,j}-\phi^{n+1}_{i,j-1}}{0.5*(\Delta y_j+\Delta y_{j-1})}+\frac{4}{3}(\bar{E}_r\tilde{v}_y)|_{i,j-\frac{1}{2}}\right)\right\}=0.
\end{aligned} \tag{4.9}$$

Based on the above Eq. (4.9), together with the discretization of the third equation of (3.1) for the fluid, we recover the numerical discretization of the third equation for the equilibrium diffusive radiation hydrodynamics (2.9).

Thirdly, multiplying the last equation of (3.12) with $\vec{\Omega}$ and integrating the resulting equation in the angular variable, with the help of the first equation of (3.12) and (4.5) we get

$$\begin{aligned}
&\rho^{n+1}_{i,j}\frac{\vec{v}^{n+1}_{i,j}-\vec{v}^{h}_{i,j}}{\Delta t}+\frac{1}{\Delta x_i}\left\{\frac{\phi^{n+1}_{i+1/2,j}+\phi^{n}_{i+1/2,j}}{6c}-\frac{\phi^{n+1}_{i-1/2,j}+\phi^{n}_{i-1/2,j}}{6c}\right\}\\
&+\frac{1}{\Delta y_j}\left\{\frac{\phi^{n+1}_{i,j+1/2}+\phi^{n}_{i,j+1/2}}{6c}-\frac{\phi^{n+1}_{i,j-1/2}+\phi^{n}_{i,j-1/2}}{6c}\right\}=0.
\end{aligned} \tag{4.10}$$

Thus, with the discretization of the second equation of (3.1) for the fluid part and the above equation (4.10), the numerical discretization of the second equation for the equilibrium diffusive radiation hydrodynamics (2.9) is recovered.

Since there is no ϵ term in the first equation of (2.1), the discretization for the first equation of (3.6) is the same mass conservation equation of (2.9). This shows that the coupled GKS and UGKS method for the system (2.1) does have the asymptotic preserving property. By virtue of (4.8), Eq. (4.9) becomes a standard five points scheme for the third (diffusion) equation of (2.9). Therefore, the current scheme can recover the diffusion solution without the constraint on the cell size being smaller than the photon's mean free path. □

Table 1 Initial condition for the Mach 1.2 radiative shock problem

Parameter	Pre-shock value	Post-shock value	Units
ρ	1.00000000e+00	1.29731782e+00	g cm^{-3}
u	1.52172533e−01	1.17297805e−01	cm sh^{-1}
T	1.00000000e−01	1.19475741e−01	keV
E_r	1.37201720e−06	2.79562228e−06	Jk cm^{-3}

Table 2 Initial condition for the Mach 3 radiative shock problem

Parameter	Pre-shock Value	Post-shock value	Units
ρ	1.00000000e+00	3.00185103e+00	g cm^{-3}
u	3.80431331e−01	1.26732249e−01	cm sh^{-1}
T	1.00000000e−01	3.66260705e−01	keV
E_r	1.37201720e−06	2.46899872e−04	Jk cm^{-3}

5 Numerical Results

In the following examples, we take the unit for length is cm, the unit for time is ns, the unit for temperature is keV and the unit for the energy is GJ. With these units, the light speed $c = 29.89cm/ns$, the radiation constant $a = 0.001372GJ/(cm^3 * keV^4)$. And we take $\theta = 0$ for the Eulerian simulation. Based on the above units, we can take $\epsilon = 1$ inthe simulation. For the angle direction, the S_4 is used for the DOM method. The maximum error for the whole nonlinear iteration is 10^{-6}, for the macro auxiliary equations is 10^{-8}, and for the radiation transfer equation is 10^{-7}. The maximum iteration number is 15 for the whole nonlinear iteration, 50 for the macro auxiliary equations, and 20 for the radiation transfer equation. Furthermore, all examples are tested on the ThinkPad X250 notebook with Inter Core i7-5600U, 8GB RAM.

Example 1 (Radiative shock) The newly developed multiscale method will be tested in two radiative shock cases, which are presented in [17,18]. For both shocks, the parameters are the monatomic gas $\gamma = 5/3$, the specific heat $c_v = 0.14472799784454\ JKkeV^{-1}g^{-1}(1JK = 10^9J)$, the total absorption coefficient $\sigma_t = 577.35cm^{-1}$, and the scattering coefficient $\sigma_s = 0$. The specifications of the conditions in the far-stream pre and post-shock regions are provided in Tables 1 and 2 for Mach 1.2 and Mach 3 shocks, respectively. The initial condition for the calculation is that on the left half of the spatial domain the pre-shock condition is adopted and on the right half of the domain the post-shock state is used. The CFL number is 0.6 and two meshes with 500 and 1000 cells are used in each calculation. The steady state solutions for both cases are obtained. For the strong shock, the material temperature reaches its maximum at the post-shock state, this point is called the Zel'dovich spike.

Case 1. (Mach 1.2 **shock)** For the weak radiative shock at Mach 1.2, the numerical results are shown in Fig. 1. There is a hydrodynamic shock, but no visible Zel'dovich spike [18]. In the numerical solution, we observe a discontinuity in the fluid temperature due to the hydrodynamic shock, and the maximum temperature is bounded by the far-downstream temperature. This matches with the results in [17,18]. The total computational time is 61 min, and there are 5000 computational steps.

Case 2. (Mach 3 **shock)** For the strong radiative shock at Mach 3, the numerical results are shown Fig. 2. Both hydrodynamic shock and Zel'dovich spike appear. Discontinuities in

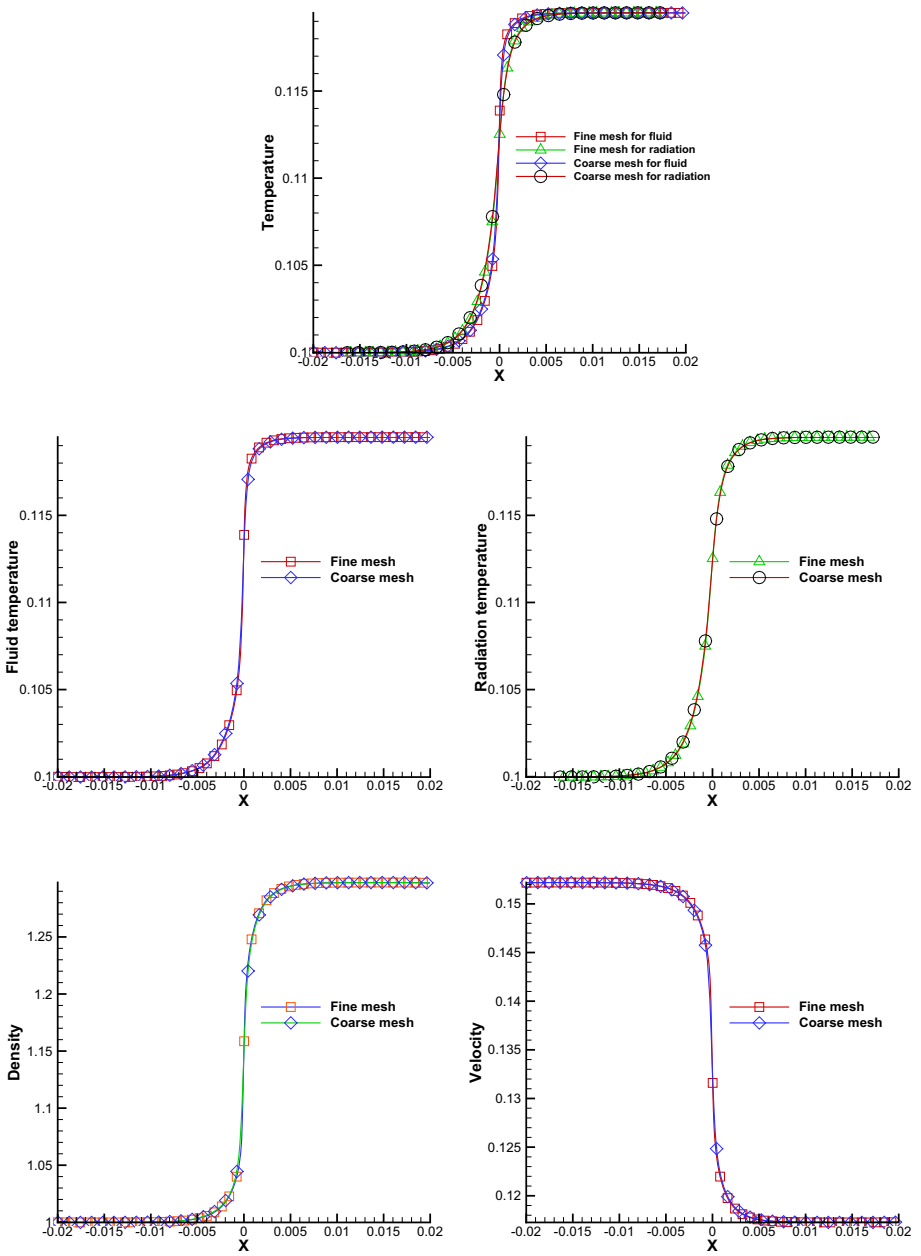

Fig. 1 Case 1 of example 1: numerical results for Mach 1.2 radiative shock

both fluid density and temperature are observed in the hydrodynamic shock. The Zel'dovich spike emerges at the shock front with enhanced fluid temperature, and leads to a relaxation region downstream where the fluid temperature and radiation temperature get to equilibrate.

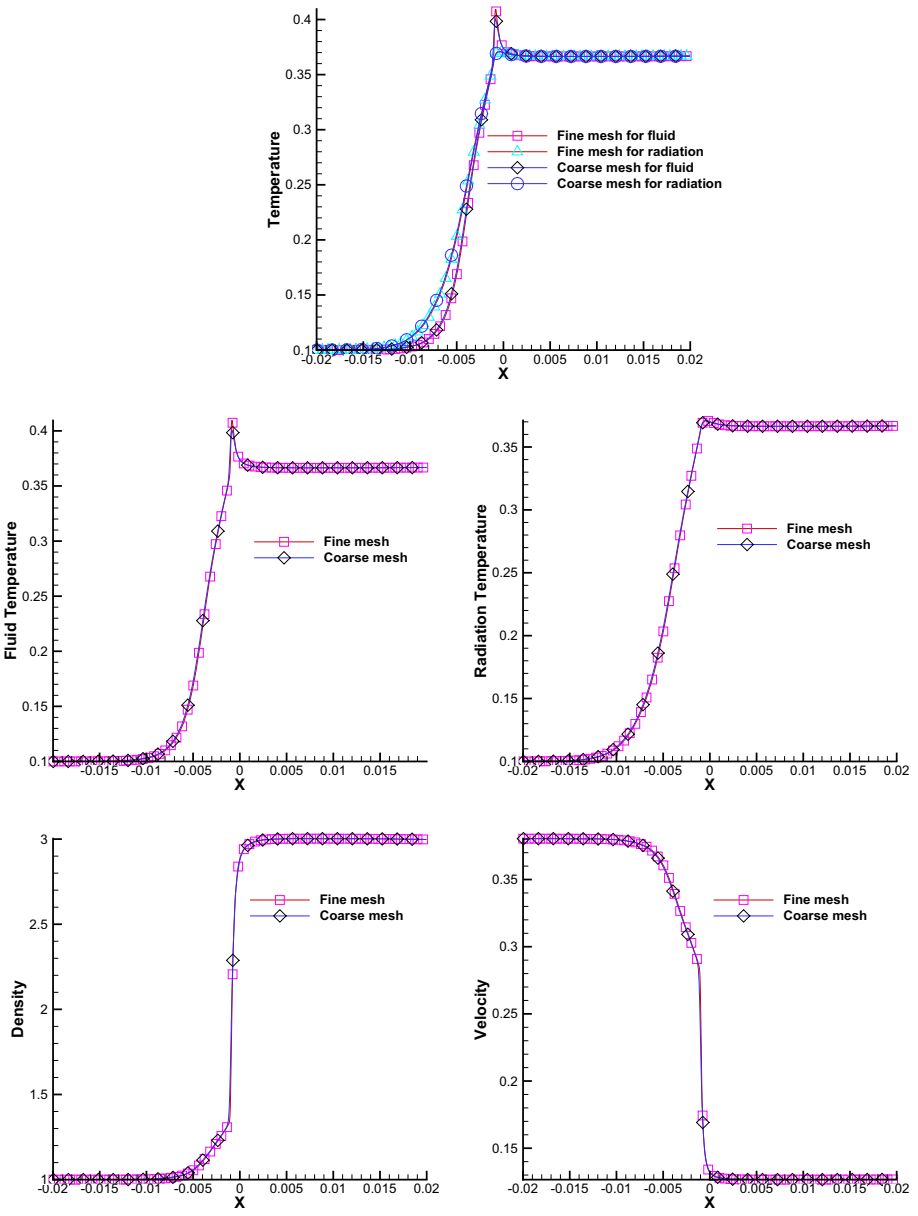

Fig. 2 Case 2 of example 1: numerical results for Mach 3 radiative shock

There is in good agreement with the results in [17,18]. The total computational time is 237 min, there are total 10^4 computational steps.

Example 2 (Interaction between a shock and a bubble) This is about a Mach 3 shock, the same as the case 2 in Example 1, interacting with a denser bubble. Initially, there is a circular bubble of radius $R = 0.2$ with its center located at $(-0.008,0.01)$ in the computational domain $[-0.02.0.4] \times [0, 0.02]$. The bubble is 25 times denser than the surrounding gas, and the

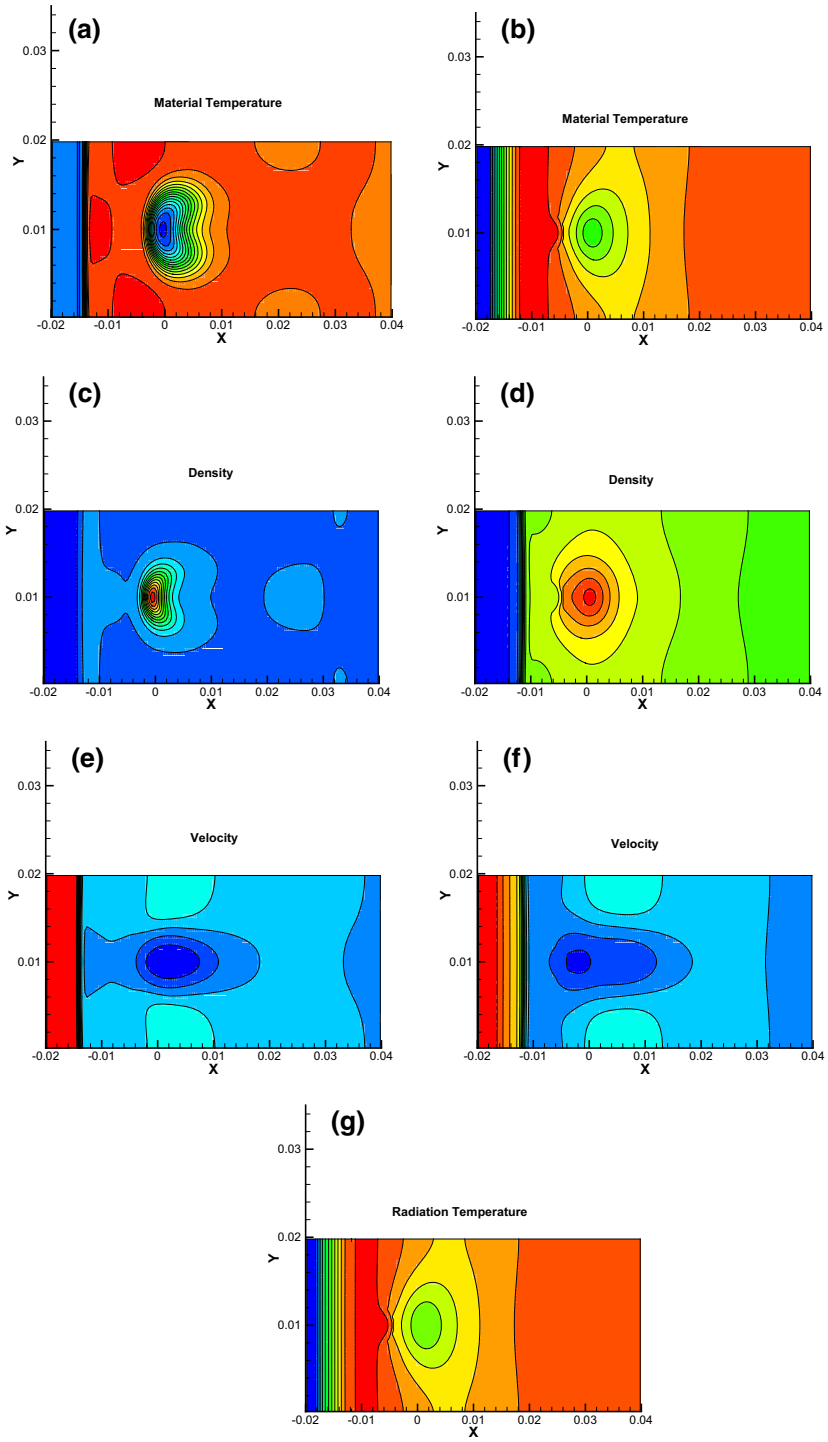

Fig. 3 Computed results at time $t = 1.4ns$ of example 2. The left figures **a**, **c**, **e** the temperature, density, and velocity of the purely Euler gas dynamic solution, while the right figures **b**, **d**, **f** the numerical results for radiation hydrodynamics. The **g** is the computed radiation temperature

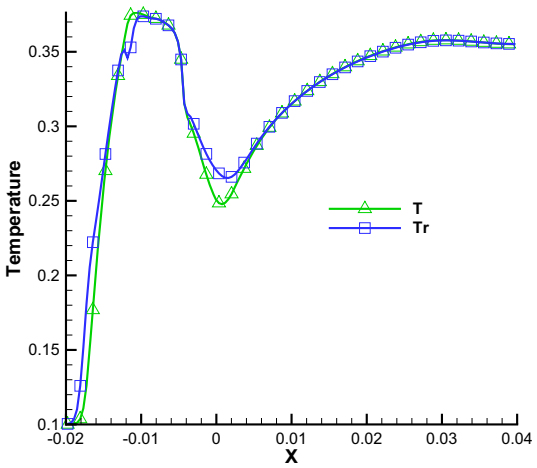

Fig. 4 Computed material and radiation temperatures at line $y = 0.01$ and time $t = 1.4ns$ in Example 2

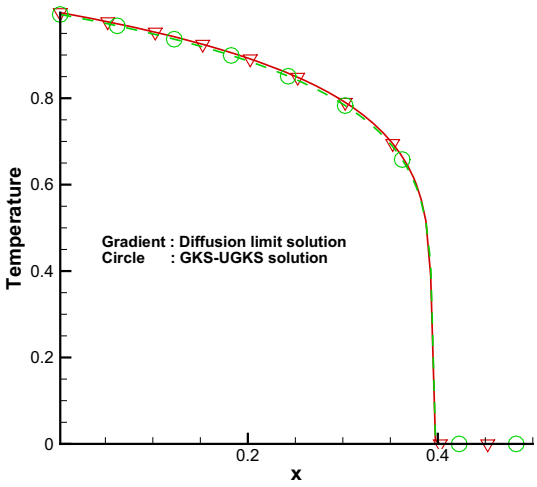

Fig. 5 Comparing material temperatures with the diffusion limit solution at time $t = 74ns$ for Example 3

opacity parameter in the bubble is 100 times of that in the ambient gas. The shock is introduced at $x = -0.012$ with the same initial pre- and post-shock states for (ρ, T, T_r, u) as given in Table 2, and the initial value for v is zero. The upper and lower boundary conditions are zero gradients for the flow variables and reflective for the radiation intensity. The radiation constant a_R and the light speed are the same as given in the first two examples. The computation is performed with 150×50 cells. The output time is $t = 1.4ns$. As a comparison, we also give the numerical solution of the Euler equations at the same output time. As shown in the Fig. 3, the phenomena of Zel'dovich spike appears at the shock front by comparing the material temperature with the radiation temperature at line $y = 0.01$ in Fig. 4. The total computational time for the radiation hydrodynamics is 208 min, where the hydrodynamic part takes 5 min only.

Example 3 (Marshak Wave-2B) In order to test the capacity of the current scheme to capture the radiative equilibrium diffusion solution in the optical thick limit, we set zero fluid velocity and keep the energy exchange between the material and radiation. The opacity coefficient

of the material is $\sigma = \frac{100}{T^3}$ cm^2/g with constant specific heat 0.1 GJ/g/keV and density 3.0 g/cm^3. The initial material temperature T is set to be 10^{-6} keV. The computational domain is a two-dimensional slab $[0, 1] \times [0, 0.01]$. A constant isotropic incident radiation intensity with a Planckian distribution at 1 keV is kept on the left boundary, and an initial constant value is set at the right boundary. In Fig. 5, the result of material temperature is compared with the the diffusion limiting solution at time 74 ns. Reasonable agreement has been obtained.

6 Conclusion

In this paper, a multiscale method for radiation hydrodynamics is developed by coupling gas dynamic movement and radiative transfer. More specifically, the scheme simulates the radiation transport through a gas dynamic system with momentum and energy exchange. For the hydrodynamic part, the GKS is used to solve the compressible flow equations, while for the radiative transfer part, the multiscale UGKS is adopted. Since both GKS and UGKS are finite volume methods, all unknowns are defined inside each cell and consistent discretizations for the hydrodynamics and radiative transfer can be constructed. Due to the multiscale nature of UGKS, the final scheme has the asymptotic preserving property for the whole system. For example, the coupled scheme can recover the equilibrium diffusion limit for the radiation transport in the optically thick gas region, and has no requirement for the cell size being less than photon's mean free path. Theoretically, accurate solution can be obtained in different optical thickness regimes. The standard radiation shock wave problems and the interaction between the shock and dense bubble have been tested to validate the proposed method. The Marshak wave problem is simulated to test the asymptotic preserving property of the scheme.

Acknowledgements The current research is supported by NSFC (No. 11671048), CAEP foundation (No. CX20200026), National key project (GJXM92579) and Science Challenge Project (No. TZ2016002) for Sun; by NSFC (Grant Nos. 11631008, GZ1465, 11571046) for Jiang; and by Hong Kong research grant council (16206617) and NSFC (Grant Nos. 11772281, 91852114) for Xu.

References

1. Mihala, D., Mihala, B.W.: Foundations of Radiation Hydrodynamics. Oxford University Press, New York (1984)
2. Lowrie, R.B., Morel, J.E., Hittinger, J.A.: The coupling of radiation and hydrodynamics. Astrophys. J. **521**, 432–450 (1999)
3. Lowrie, R.B., Wollaber, A.B.: Simple material-motion corrections for thermal radiactive transport. In: 23rd International Conference on Transport Theory, Santa Fe, NM, USA, 15–20 September 2013
4. McClarren, R.G., Evans, T.M., Lowrie, R.B., Densmore, J.D.: Semi-implicit time integration for Pn thermal radiative transfer. J. Comput. Phys. **227**, 7561–7586 (2008)
5. Lowrie, R.B.: A comparison of implicit time integration methods for nonlinear relaxation and diffusion. J. Comput. Phys. **196**, 566–590 (2004)
6. Knoll, D.A., Lowrie, R.B., Morel, J.E.: Numerical analysis of time integration errors for nonequilibrium radiation diffusion. J. Comput. Phys. **226**, 1332–1347 (2007)
7. Olson, G.L.: Second-order time evolution of Pn equations for radiation transport. J. Comput. Phys. **228**, 3027–3083 (2009)
8. Axelrod, T.S., Dubois, P.F., Rhoades Jr., C.E.: An implicit scheme for calculating time- and fequency-dependent flux limited radiation diffusion in one dimension. J. Comput. Phys. **54**, 205–220 (1984)
9. Stone, J.M., Mihalas, D.: Upwind monotonic interpolation methods for the solution of the time dependent radiative transfer equation. J. Comput. Phys. **100**, 402–408 (1992)
10. Brown, P.N., Shumaker, D.E., Woodward, C.S.: Fully implicit solution of large-scale non-equilibrium radiation diffusion with high order time integration. J. Comput. Phys. **204**, 760–783 (2005)

11. Sun, W.J., Jiang, S., Xu, K.: An asymptotic preserving unified gas kinetic scheme for gray radiative transfer equations. J. Comput. Phys. **285**, 265–279 (2015)
12. Sun, W.J., Jiang, S., Xu, K., Li, S.: An asymptotic preserving unified gas kinetic scheme for frequency-dependent radiative transfer equations. J. Comput. Phys. **302**, 222–238 (2015)
13. Sun, W.J., Jiang, S., Xu, K.: An implicit unified gas kinetic scheme for radiative transfer with equilibrium and non-equilibrium diffusive limits. Commun. Comput. Phys. **22**, 899–912 (2017)
14. Toro, E.: Riemann Solvers and Numerical Methods for Fluid Dynamics: A Practical Introduction. Springer, New York (1999)
15. Xu, K.: A gas-kinetic BGK scheme for the Navier–Stokes equations and its connection with artifical dissipation and Godunov method. J. Comput. Phys. **171**, 289–335 (2001)
16. Kadioglu, S.Y., Knoll, D.A., Lowrie, R.B., Rauenzahn, R.M.: A second order self-consistent IMEX method for radiation hydrodynamics. J. Comput. Phys. **229**, 8313–8332 (2010)
17. Bolding, S., Hansel, J., Edwards, J.D., Morel, J.E., Lowrie, R.B.: Second-order discretization in space and time for radiation-hydrodynamics. J. Comput. Phys. **32**, 101–136 (2017)
18. Lowrie, R.B., Edwards, J.D.: Radiative shock solutions with grey non-equillibrium diffusion. Shock Waves **18**, 129–143 (2008)
19. Dai, W., Woodward, P.R.: Numerical simulations for radiation hydrodynamics. I. Diffusion limit. J. Comput. Phys. **142**, 182–207 (1998)
20. Bates, J.W., Knoll, D.A., Rider, W.J., Lowrie, R.B., Mousseau, V.A.: On consistent time-integration methods for radiation hydrodynamics in the equilibrium diffusion limit: low-energy-density regime. J. Comput. Phys. **167**, 99–130 (2001)
21. Sun, W.J., Jiang, S., Xu, K.: A multidimensional unified gas-kinetic scheme for radiative transfer equations on unstructured mesh. J. Comput. Phys. **351**, 455–472 (2017)
22. Xu, K.: Direct Modeling for Computational Fluid Dynamics: Construction and Application of Unified Gas Kinetic Schemes. World Scientific, Singapore (2015)
23. Xu, K.: A gas-kinetic BGK scheme for the Navier–Stokes equations and its connection with artificial dissipation and Godunov method. J. Comput. Phys. **171**, 289–335 (2001)
24. Sekora, M., Stone, J.: A higher order godunov method for radiation hydrodynamics: radiation subsystem. Commun. Appl. Comput. Math. **4**, 135–152 (2009)
25. Bhatnagar, P.L., Gross, E.P., Krook, M.: A model for collision processes in gases I: small amplitude processes in charged and neutral one-component systems. Phys. Rev. **94**, 511–525 (1954)
26. van Leer, B.: Towards the ultimate conservative difference schemes V. A second-order sequal to Godunov's method. J. Comput. Phys. **32**, 101–136 (1979)
27. Chandrasekhar, S.: Radiative Transfer. Dover Publications, Mineola (1960)
28. Xu, K., Huang, J.C.: A unified gas-kinetic scheme for continuum and rarefied flows. J. Comput. Phys. **229**, 7747–7764 (2010)